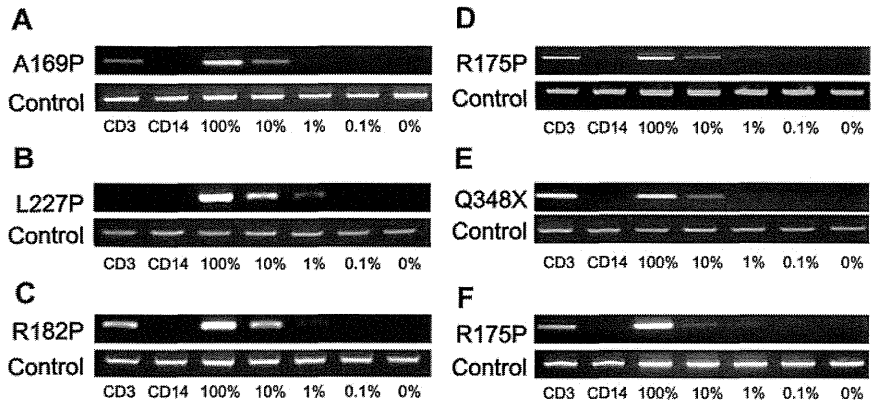

Figure 4. NEMO reversion selectively occurs in T cells of XL-EDA-ID patients. Allele-specific PCR for *NEMO* on $CD3^+$ or $CD14^+$ cells from (A) patient 4, (B) patient 5, (C) patient 6, (D) patient 7, (E) patient 8, and (F) patient 9. Numbers below each figure indicate the percentages of wild-type NEMO cDNA mixed with each mutant. Primers used in each PCR are shown on the left.

concordance between the degree of the disruption of *NEMO* gene and the proportion of reverted $NEMO^{normal}$ cells compared with $NEMO^{low}$ cells. The high proportion of reverted T cells seen in patients 1 and 2 as well as in patient 8 was associated with a highly disruptive mutation of the *NEMO* gene (ie, a duplication mutation in patients 1 and 2, and a truncation mutation in patient 8). In addition, the highly selective X-chromosome inactivation observed in the mothers of XL-EDA-ID patients indicated a strong selective advantage for $NEMO^{normal}$ cells over $NEMO^{low}$ cells. It is also noteworthy that reverted T cells were not detected in patient 5, who carried an L227P mutation that was not localized to either of the functional domains in the NEMO protein. Other reported cases with the same mutation presented with polysaccharide-specific humoral immunodeficiency and autoinflammatory diseases, but were spared complications such as cellular immunodeficiency and susceptibility to *Mycobacterium* (similar to patient 5).[4,8] This may reflect the fact that the L227P mutation in NEMO has less influence on T-cell growth than NEMO mutations that occur in functional domains, and suggests that reversion of the mutation has little impact on T-cell survival. Although the number of cases in our study is limited, it appears that the more disruptive NEMO mutations favor the survival of $NEMO^{normal}$ cells after reversion and X-chromosome inactivation.

Regarding the gradual decline in the number of NEMO-deficient T cells, one candidate trigger could be infection. Because the dominance of the memory phenotype and the skewed TCR repertoire among $CD8^+$ T cells in $NEMO^{normal}$ cells were observed in both patients 1 and 2 (Figure 1C and Mizukami et al[18]), continuous infection of pyogenic bacteria in patient 1 and *M szulgai* in patient 2 could be a reason for the emergence of $NEMO^{normal}$ cells and the elimination of $NEMO^{low}$ cells. The decrease in $NEMO^{normal}$ cells and restoration of $NEMO^{low}$ cells after anti-mycobacterial therapy in patient 2 support this hypothesis. In the case of patient 1, the predominance of $NEMO^{normal}$ T cells with an effector/memory phenotype at diagnosis (Table 4 and Mizukami et al[18]) is likely to be the result of chronic infection, and it is possible that $NEMO^{low}$ cells were predominant during his early infancy. Because some reports have indicated that TNF-α–induced programmed cell death of several cell types, including a human T-cell line, was enhanced by hypomorphic *NEMO* mutations,[12,35] and considering our finding that the levels of TNF-α expressed in revertant T cells were similar to levels in healthy control T cells in vitro (Figure 1F), TNF-α produced from these cells in response to infection could be involved in mutant T-cell elimination.

Unexpectedly, T-cell proliferation in patient 2 was equivalent to that of normal controls at the age of 2 months and was reduced after $NEMO^{normal}$ T cells increased (Figure 1B; Table 3). This finding indicates that the $NEMO^{low}$ T cells did not have intrinsically impaired mitogen-induced proliferation. One reasonable explanation for the reduced proliferation observed after the increase in $NEMO^{normal}$ T cells is a reduction in the absolute number of T cells (naive T cells in particular), probably because of the infection.

Table 5. Expression of mutant NEMO in various cell lineages for the mother of each XL-EDA-ID patient

Sample	Mutation	Analysis	Subtype	Mutant type, % (proportion)
Mother of patients 1 and 2	Duplication	FACS	CD3	0
			CD14	0
			CD19	0
Mother of patient 3	D311E	FACS	CD3	13
			$CD3^-$	54
		Subcloning	CD3	22 (6/27)
			$CD3^-$	55 (12/22)
Mother of patient 4	A169P	Subcloning	CD3	52 (11/21)
			CD14	58 (11/19)
			CD19	42 (5/12)
Mother of patient 8	Q348X	Subcloning	CD3	0 (0/26)
			CD14	17 (3/18)
			CD19	0 (0/18)
Mother of patient 10	1167insC	Subcloning	CD3	18 (7/39)
			CD14	12 (5/43)
			CD19	27 (12/44)

Data are shown as either the percentages of $NEMO^{normal}$ cells, as assessed by flow cytometry, or as the ratio of clones containing wild-type NEMO to the total number of clones, as analyzed by subcloning and sequencing analysis.

Table 6. Expression of mutant NEMO in CD3-positive cells and PHA blasts

Sample	Mutations	Analysis	Subtype	Mutant type, % (proportion)
Mother of patient 3	D311E	FACS	CD3	13
			PHA blast	47
		Subcloning	CD3	22 (6/27)
			PHA blast	48 (11/23)
Mother of patient 4	A169P	Subcloning	CD3	52 (11/21)
			PHA blast	18 (9/49)
Mother of patient 8	Q348X	Subcloning	CD3	0 (0/26)
			PHA blast	0 (0/21)
Mother of patient 10	1167insC	Subcloning	CD3	18 (7/39)
			PHA blast	9 (4/43)
Patient 2	Duplication	FACS	CD3	73
			PHA blast	93
Patient 4	A169P	Subcloning	CD3	79 (19/24)
			PHA blast	100 (37/37)
Patient 8	Q348X	Subcloning	CD3	56 (18/32)
			PHA blast	100 (16/16)
Patient 9	R175P	Subcloning	CD3	87 (34/39)
			PHA blast	0 (0/28)

PHA blasts were obtained by incubating PBMCs with PHA and soluble IL-2 for 7 days. Data are shown as either the percentages of $NEMO^{normal}$ cells, as assessed by flow cytometry, or as the ratio of clones containing wild-type NEMO to the total number of clones, as analyzed by subcloning and sequencing analysis.

Therefore, to identify other mechanisms underlying reduced T-cell proliferation, the impact of *NEMO* mutation on PHA-induced T-cell proliferation was indirectly examined in vitro by comparing the response of $NEMO^{normal}$ and $NEMO^{low}$ cells derived from XL-EDA-ID patients and their mothers. After PHA stimulation and proliferation, the proportion of $NEMO^{low}$ T cells increased in patients 2, 4, and 8, while the opposite result was observed in patient 9 and in the mother of patient 4 (Table 6). Although the precise mechanism is unclear, a reduction in the proportion of $NEMO^{normal}$ cells after PHA stimulation would reflect the lower proliferative capacity of $NEMO^{normal}$ cells compared with that of $NEMO^{low}$ cells, which may be another explanation for the reduced T-cell proliferation observed in patient 2 at 23 months of age when $NEMO^{normal}$ T cells were dominant. In the reports on reversion mosaicism of *IL2RG* gene mutations,[28,36] the restoration of T-cell function and clinical symptoms varied among patients. Therefore, other factors besides the genotype of the mutations, such as the developmental stage where reversion occurred and the frequency of reversion, affect the clinical impact of somatic mosaicism of *NEMO* gene mutations.

In this study, the effect of somatic mosaicism of the *NEMO* gene on clinical phenotype could not be fully evaluated. However, cytokines produced by revertant T cells could influence the development of clinical symptoms of XL-EDA-ID, such as inflammatory bowel disease. In a mouse model, intestinal epithelial cell-specific inhibition of NF-κB through the conditional ablation of NEMO resulted in the development of chronic bowel inflammation sensitized intestinal epithelial cells to TNF-α–induced apoptosis.[37] In this model, the first phase of intestinal inflammation was initiated by epithelial cell death and was followed by a second phase of TNF-α–induced intestinal inflammation, the latter being dependent on T cells. Another report showed that HSCT in XL-EDA-ID patients exacerbated the patients' inflammatory bowel disease.[38] Indeed, in patient 4, the percentage of reverted T cells was reduced after repeated administrations of anti-TNFα blocking Ab, and the symptoms of inflammatory bowel disease improved.[18] Considering this evidence, somatic mosaicism in T cells might be an important factor leading to inflammatory disease in XL-EDA-ID patients with defective NF-κB activation. However, our study did not show a tight association between inflammatory bowel disease and somatic mosaicism, and further investigation is needed to determine whether the $NEMO^{normal}$ T cells play a role in inflammatory processes in XL-EDA-ID.

In conclusion, this study has identified a high frequency of somatic mosaicism in XL-EDA-ID patients, particularly in T cells, and has revealed important insights into human T-cell immunobiology in XL-EDA-ID. Although we could not demonstrate the clinical impact of somatic mosaicism in XL-EDA-ID patients, our findings suggest that care is required when making molecular diagnoses of XL-EDA-ID, and might shed light on the mechanisms underlying the variability in the clinical manifestation of XL-ED-ID and facilitate the search for appropriate treatments.

Acknowledgments

The authors are grateful to all the XL-EDA-ID patients and their families for their participation. They also thank Shoji Yamaoka (Department of Molecular Virology, Graduate School of Medicine, Tokyo Medical and Dental University, Tokyo, Japan) for kindly providing NEMO-null rat fibroblast cells, and Takeda Pharmaceutical Company Limited for kindly providing the recombinant human IL-2.

This work was supported by grants from the Japanese Ministry of Education, Culture, Sports, Science, and Technology, and by grants from the Japanese Ministry of Health, Labor and Welfare.

Authorship

Contribution: Tomoki Kawai wrote the manuscript and performed research; R.N., T.Y., T.N., and T.H. edited the manuscript and supervised this work; K.I., Y.M., N.T., H.S., M.S., and Y.T. cultured cells; and T. Mizukami, H.N., Y.K., A.Y., T. Murata, S.S., E.I., H.A., Toshinao Kawai, C.I., S.O., and M.K. treated patients and analyzed data.

Conflict-of-interest disclosure: The authors declare no competing financial interests.

Correspondence: Ryuta Nishikomori, MD, PhD, Department of Pediatrics, Kyoto University Graduate School of Medicine, 54 Kawahara-cho, Shogoin, Sakyo-ku, Kyoto 606-8507, Japan; e-mail: rnishiko@kuhp.kyoto-u.ac.jp.

References

1. Pinheiro M, Freire-Maia N. Ectodermal dysplasias: a clinical classification and a causal review. *Am J Med Genet.* 1994;53(2):153-162.
2. Abinun M, Spickett G, Appleton AL, Flood T, Cant AJ. Anhidrotic ectodermal dysplasia associated with specific antibody deficiency. *Eur J Pediatr.* 1996;155(2):146-147.
3. Sitton JE, Reimund EL. Extramedullary hematopoiesis of the cranial dura and anhidrotic ectodermal dysplasia. *Neuropediatrics.* 1992;23(2):108-110.
4. Schweizer P, Kalhoff H, Horneff G, Wahn V, Diekmann L. [Polysaccharide specific humoral immunodeficiency in ectodermal dysplasia. Case report of a boy with two affected brothers]. *Klin Padiatr.* 1999;211(6):459-461.
5. Abinun M. Ectodermal dysplasia and immunodeficiency. *Arch Dis Child.* 1995;73(2):185.
6. Zonana J, Elder ME, Schneider LC, et al. A novel X-linked disorder of immune deficiency and hypohidrotic ectodermal dysplasia is allelic to incontinentia pigmenti and due to mutations in IKK-gamma (NEMO). *Am J Hum Genet.* 2000;67(6):1555-1562.
7. Courtois G, Smahi A, Israel A. NEMO/IKK gamma: linking NF-kappa B to human disease. *Trends Mol Med.* 2001;7(10):427-430.
8. Doffinger R, Smahi A, Bessia C, et al. X-linked anhidrotic ectodermal dysplasia with immunodeficiency is caused by impaired NF-kappaB signaling. *Nat Genet.* 2001;27(3):277-285.
9. Rothwarf DM, Zandi E, Natoli G, Karin M. IKK-gamma is an essential regulatory subunit of the IkappaB kinase complex. *Nature.* 1998;395(6699):297-300.
10. Yamaoka S, Courtois G, Bessia C, et al. Complementation cloning of NEMO, a component of the IkappaB kinase complex essential for NF-kappaB activation. *Cell.* 1998;93(7):1231-1240.
11. Smahi A, Courtois G, Vabres P, et al. Genomic rearrangement in NEMO impairs NF-kappaB activation and is a cause of incontinentia pigmenti. The International Incontinentia Pigmenti (IP) Consortium. *Nature.* 2000;405(6785):466-472.
12. Hanson EP, Monaco-Shawver L, Solt LA, et al. Hypomorphic nuclear factor-kappaB essential modulator mutation database and reconstitution system identifies phenotypic and immunologic diversity. *J Allergy Clin Immunol.* 2008;122(6):1169-1177.
13. Orange JS, Jain A, Ballas ZK, Schneider LC, Geha RS, Bonilla FA. The presentation and natural history of immunodeficiency caused by nuclear factor kappaB essential modulator mutation. *J Allergy Clin Immunol.* 2004;113(4):725-733.
14. Jain A, Ma CA, Liu S, Brown M, Cohen J, Strober W. Specific missense mutations in NEMO result in hyper-IgM syndrome with hypohydrotic ectodermal dysplasia. *Nat Immunol.* 2001;2(3):223-228.
15. Orange JS, Brodeur SR, Jain A, et al. Deficient natural killer cell cytotoxicity in patients with IKK-gamma/NEMO mutations. *J Clin Invest.* 2002;109(11):1501-1509.
16. Sebban H, Courtois G. NF-kappaB and inflammation in genetic disease. *Biochem Pharmacol.* 2006;72(9):1153-1160.
17. Nishikomori R, Akutagawa H, Maruyama K, et al. X-linked ectodermal dysplasia and immunodeficiency caused by reversion mosaicism of NEMO reveals a critical role for NEMO in human T-cell development and/or survival. *Blood.* 2004;103(12):4565-4572.
18. Mizukami T, Obara M, Nishikomori R, et al. Successful treatment with infliximab for inflammatory colitis in a patient with X-linked anhidrotic ectodermal dysplasia with immunodeficiency. *J Clin Immunol.* 2012;32(1):39-49.
19. Imamura M, Kawai T, Okada S, et al. Disseminated BCG infection mimicking metastatic nasopharyngeal carcinoma in an immunodeficient child with a novel hypomorphic NEMO mutation. *J Clin Immunol.* 2011;31(5):802-810.
20. Tono C, Takahashi Y, Terui K, et al. Correction of immunodeficiency associated with NEMO mutation by umbilical cord blood transplantation using a reduced-intensity conditioning regimen. *Bone Marrow Transplant.* 2007;39(12):801-804.
21. Saito M, Nishikomori R, Kambe N, et al. Disease-associated CIAS1 mutations induce monocyte death, revealing low-level mosaicism in mutation-negative cryopyrin-associated periodic syndrome patients. *Blood.* 2008;111(4):2132-2141.
22. Yang TP, Stout JT, Konecki DS, Patel PI, Alford RL, Caskey CT. Spontaneous reversion of novel Lesch-Nyhan mutation by HPRT gene rearrangement. *Somat Cell Mol Genet.* 1988;14(3):293-303.
23. Zhang LH, Jenssen D. Reversion of the hprt mutant clone SP5 by intrachromosomal recombination. *Carcinogenesis.* 1992;13(4):609-615.
24. Monnat RJ Jr, Chiaverotti TA, Hackmann AF, Maresh GA. Molecular structure and genetic stability of human hypoxanthine phosphoribosyltransferase (HPRT) gene duplications. *Genomics.* 1992;13(3):788-796.
25. Rautenstrauss B, Liehr T, Fuchs C, et al. Mosaicism for Charcot-Marie-Tooth disease type 1A: onset in childhood suggests somatic reversion in early developmental stages. *Int J Mol Med.* 1998;1(2):333-337.
26. Wada T, Candotti F. Somatic mosaicism in primary immune deficiencies. *Curr Opin Allergy Clin Immunol.* 2008;8(6):510-514.
27. Ariga T, Kondoh T, Yamaguchi K, et al. Spontaneous in vivo reversion of an inherited mutation in the Wiskott-Aldrich syndrome. *J Immunol.* 2001;166(8):5245-5249.
28. Stephan V, Wahn V, Le Deist F, et al. Atypical X-linked severe combined immunodeficiency due to possible spontaneous reversion of the genetic defect in T cells. *N Engl J Med.* 1996;335(21):1563-1567.
29. Rieux-Laucat F, Hivroz C, Lim A, et al. Inherited and somatic CD3zeta mutations in a patient with T-cell deficiency. *N Engl J Med.* 2006;354(18):1913-1921.
30. Wada T, Toma T, Okamoto H, et al. Oligoclonal expansion of T lymphocytes with multiple second-site mutations leads to Omenn syndrome in a patient with RAG1-deficient severe combined immunodeficiency. *Blood.* 2005;106(6):2099-2101.
31. Hirschhorn R. In vivo reversion to normal of inherited mutations in humans. *J Med Genet.* 2003;40(10):721-728.
32. Wada T, Schurman SH, Jagadeesh GJ, Garabedian EK, Nelson DL, Candotti F. Multiple patients with revertant mosaicism in a single Wiskott-Aldrich syndrome family. *Blood.* 2004;104(5):1270-1272.
33. Stewart DM, Candotti F, Nelson DL. The phenomenon of spontaneous genetic reversions in the Wiskott-Aldrich syndrome: a report of the workshop of the ESID Genetics Working Party at the XIIth Meeting of the European Society for Immunodeficiencies (ESID). Budapest, Hungary October 4-7, 2006. *J Clin Immunol.* 2007;27(6):634-639.
34. Davis BR, Yan Q, Bui JH, et al. Somatic mosaicism in the Wiskott-Aldrich syndrome: molecular and functional characterization of genotypic revertants. *Clin Immunol.* 2010;135(1):72-83.
35. Yamaoka S, Inoue H, Sakurai M, et al. Constitutive activation of NF-kappa B is essential for transformation of rat fibroblasts by the human T-cell leukemia virus type I Tax protein. *EMBO J.* 1996;15(4):873-887.
36. Speckmann C, Pannicke U, Wiech E, et al. Clinical and immunologic consequences of a somatic reversion in a patient with X-linked severe combined immunodeficiency. *Blood.* 2008;112(10):4090-4097.
37. Nenci A, Becker C, Wullaert A, et al. Epithelial NEMO links innate immunity to chronic intestinal inflammation. *Nature.* 2007;446(7135):557-561.
38. Fish JD, Duerst RE, Gelfand EW, Orange JS, Bunin N. Challenges in the use of allogeneic hematopoietic SCT for ectodermal dysplasia with immune deficiency. *Bone Marrow Transplant.* 2009;43(3):217-221.

bjh research paper

Identification of the integrin β3 L718P mutation in a pedigree with autosomal dominant thrombocytopenia with anisocytosis

Yoshiyuki Kobayashi,[1,2] Hirotaka Matsui,[1]* Akinori Kanai,[1] Miyuki Tsumura,[2] Satoshi Okada,[2] Mizuka Miki,[2] Kazuhiro Nakamura,[2] Shinji Kunishima,[3] Toshiya Inaba[1] and Masao Kobayashi[2]

[1]Department of Molecular Oncology and Leukaemia Programme Project, Research Institute for Radiation Biology and Medicine, Hiroshima University, [2]Department of Paediatrics, Graduate School of Biomedical and Health Sciences, Hiroshima University, Minami-ku, Hiroshima, and [3]Department of Advanced Diagnosis, Clinical Research Centre, National Hospital Organization Nagoya Medical Centre, Nagoya, Aichi, Japan

Received 29 June 2012; accepted for publication 22 October 2012

Correspondence: Hirotaka Matsui, Department of Molecular Oncology and Leukemia Program Project, Research Institute for Radiation Biology and Medicine, Hiroshima University, 1-2-3 Kasumi, Minami-ku, Hiroshima 734-8553, Japan.
E-mail: hmatsui@hiroshima-u.ac.jp

Summary

αIIbβ3 integrin mutations that result in the complete loss of expression of this molecule on the platelet surface cause Glanzmann thrombasthenia. This is usually autosomal recessive, while other mutations are known to cause dominantly inherited macrothrombocytopenia (although such cases are rare). Here, we report a 4-generation pedigree including 10 individuals affected by dominantly inherited thrombocytopenia with anisocytosis. Six individuals, whose detailed clinical and laboratory data were available, carried a non-synonymous *ITGB3* gene alteration resulting in mutated integrin β3 (ITGB3)-L718P. This mutation causes partial activation of the αIIbβ3 complex, which promotes the generation of abnormal pro-platelet-like protrusions through downregulating RhoA (RHOA) activity in transfected Chinese Hamster Ovary cells. These findings suggest a model whereby the integrin β3-L718P mutation contributes to thrombocytopenia through gain-of-function mechanisms.

Keywords: integrin β3 L718P mutation, familial thrombocytopenia, autosomal dominant inheritance, whole exome sequencing, inhibition of RhoA.

Lifelong haemorrhagic syndromes are in part caused by point mutations in the *ITGA2B* and *ITGB3* genes encoding ITGA2B and ITGB3 proteins (integrin αIIb and β3, respectively). The αIIbβ3 complex regulates thrombopoiesis by megakaryocytes and aggregation of platelets in response to extracellular stimuli, such as ADP and collagen. The autosomal recessive syndrome, Glanzmann thrombasthenia, is the most frequently encountered disease caused by αIIbβ3 mutations (George *et al*, 1990; Nurden, 2006; Nurden & Nurden, 2008; Nurden *et al*, 2011a). Patients have a homozygous or a compound heterozygous mutation in the *ITGA2B* or *ITGB3* genes that causes loss of function of the αIIbβ3 complex. Although platelet counts and size are generally normal, patients typically have severe mucocutaneous bleeding, such as epistaxis, menorrhagia and gastrointestinal bleeding, frequently because of defects in platelet aggregation.

Mutations of the αIIbβ3 complex are also involved in congenital haemorrhagic diseases other than Glanzmann thrombasthenia (Ghevaert *et al*, 2008; Schaffner-Reckinger *et al*, 2009; Jayo *et al*, 2010; Kunishima *et al*, 2011; Nurden *et al*, 2011b). For example, the integrin β3 D723H mutation is found in autosomal dominant macrothrombocytopenia (Ghevaert *et al*, 2008). Biochemical analysis revealed that integrin β3-D723H is a gain of function mutation which activates the αIIbβ3 complex constitutively, albeit only partially. This results in the formation of proplatelet-like protrusions in transfected Chinese Hamster Ovary (CHO) cells, a model of relevance for the formation of macrothrombocytes (Ghevaert *et al*, 2008; Schaffner-Reckinger *et al*, 2009).

More recently, a sporadic patient carrying an integrin β3-L718P mutation was reported (Jayo *et al*, 2010). She had mild thrombocytopenia (127×10^9/l), platelet anisocytosis and reduced platelet aggregation potential. This mutation also induces abnormal proplatelet formation.

In the present study, we report a pedigree with a total 10 of individuals affected by a dominantly inherited haemorrhagic

First published online 17 December 2012
doi:10.1111/bjh.12160

syndrome. Six individuals whose detailed clinical and laboratory data are available, presented with thrombocytopenia accompanied by anisocytosis and carry a non-synonymous *ITGB3* T2231C alteration resulting in the integrin β3-L718P mutation. We also performed entire exon sequencing by a next-generation sequencing and found that the integrin β3-L718P mutation is most likely the sole gene responsible for thrombocytopenia in this pedigree.

Materials and methods

Written informed consent was obtained from individuals in the family in accordance with the Declaration of Helsinki for blood sampling and analysis undertaken with the approval of the Hiroshima University Institutional Review Board.

Patient

The patient was 4-year-old Japanese girl (iv.3 in Fig 1A), who presented with mild bleeding tendencies, such as recurrent nasal bleeding and purpura in her extremities. Her platelet count was 49–72 × 10^9/l with a mean platelet volume (MPV) of 9·8–10·9 fl. White blood cell and red blood cell counts were within the normal range and there were no morphological abnormalities including inclusions in neutrophils. Bone marrow examination was not performed. A total of six of her relatives, namely her father (iii.2), sister and brother (iv.1 and iv.2), two cousins (iv.4 and iv.5) and an aunt (iii.5), were subsequently found to have low platelet counts and were referred to our institute for further investigation.

Antibodies and reagents

Unconjugated or phycoerythrin-cyanin 5 (PC5)-conjugated anti-CD41 monoclonal antibody (Ab) (clone P2) against the αIIbβ3 complex (Beckman Coulter, Brea, CA, USA), fluorescein isothiocyanate (FITC)-conjugated anti-CD41a monoclonal Ab (clone HIP8) (Beckman Coulter), FITC- or peridinin chlorophyll (PerCP)-conjugated anti-CD61 monoclonal Ab (clone RUU-PL 7F12) (BD Biosciences, San Jose, CA, USA), FITC-conjugated PAC-1 (BD Biosciences) and Alexa488-conjugated human fibrinogen (Life Technologies, Carlsbad, CA, USA) were used in flow cytometry. Anti-CD61 monoclonal Ab (clone EP2417Y) (Abcam, Cambridge, UK), anti-DDDDK-tag polyclonal Ab (Medical & Biological Laboratories, Nagoya, Japan), Alexa488-conjugated phalloidin and Hoechst 33342 (both Life Technologies) were used for immunofluorescence microscopy. The oligopeptide Arg-Gly-Asp-Ser (RGDS) (Sigma–Aldrich, St Louis, MO, USA) was used to competitively inhibit the binding of ligands to αIIbβ3, and adenosine diphosphate (ADP) (nacalai tesque, Kyoto, Japan) was used for the stimulation of αIIbβ3 on platelets.

Construction and transfection of expression vectors

Full-length wild type (WT) *ITGA2B* and *ITGB3* cDNA were amplified by polymerase chain reaction (PCR) and cloned into pcDNA3·1 expression vectors. A PCR-mediated site-directed mutagenesis technique was applied to produce *ITGB3* mutants encoding integrin β3-L718P, -D723H and -T562N with or without truncation at the C-terminal side of Y^{759} (del. 759). *RHOA* cDNA, which encodes RhoA (RHOA) protein, was amplified by PCR and its mutants (T19N and Q63L) were generated by site-directed mutagenesis, followed by cloning into p3xFLAG-CMV-10 vectors (Sigma–Aldrich). The *ITGA2B* and *ITGB3* expression vectors were simultaneously transfected into CHO cells cultured in Ham's F12 medium supplemented with 10% fetal bovine serum at 37°C, in 5% CO_2, using Lipofectamine LTX reagent (Life Technologies) according to the manufacturer's instructions.

Immunofluorescent laser-scanning confocal microscopy

Cells grown on coverslips coated with 100 μg/ml fibrinogen were fixed with 4% paraformaldehyde, followed by permeabilization with phosphate-buffered saline containing 0·1% Triton X100. After blocking, the cells were stained with primary antibodies at appropriate dilutions, followed by staining with Alexa488- or Cy3-conjugated secondary antibodies together with Hoechst 33342. High-resolution immunofluorescent images were taken under a laser-scanning confocal microscopy (LSM5 Pascal, Carl Zeiss, Oberkochen, Germany) using a x63 objective.

Flow cytometry

The expression and activation of integrin αIIb and β3 on the platelet surface was indirectly estimated by flow cytometry with the antibodies described above. Mean fluorescence intensity (MFI) of values in an affected individual were divided by those in an unrelated normal control and recorded as relative MFI value (%). For the quantitative determination of αIIbβ3 molecules on the platelet surface, QIFIKIT (Dako, Glostrup, Denmark) was used according to the manufacturer's instructions. MFI of the calibration beads containing five populations (antibody-binding capacity: 2600, 9900, 46 000, 221 000 and 741 000) were 16·12, 63·83, 262·84, 1483·2 and 3772·1, respectively, whereas that of the negative control sample was 1·62. Therefore, αIIbβ3 molecules (copies/platelet) was calculated as $10^{(1.022 \times \log(\mathrm{MFI}) + 2.1679)} - 241$. Activation of platelets and CHO cells was estimated by methods previously described (Shattil *et al*, 1987; Hughes *et al*, 1996). Activation index was defined as $(F-F_0) / (F'-F_0)$, where F is the MFI of PAC-1-stained CHO cells transfected with αIIbβ3-L718P or αIIbβ3-D723H, and F_0 and F' are those transfected with αIIbβ3-WT and αIIbβ3-T562N, respectively. The samples were analyzed on a FACS Calibur (Becton Dickinson, Franklin Lakes, NJ, USA), equipped with an argon laser operating at 488 nm.

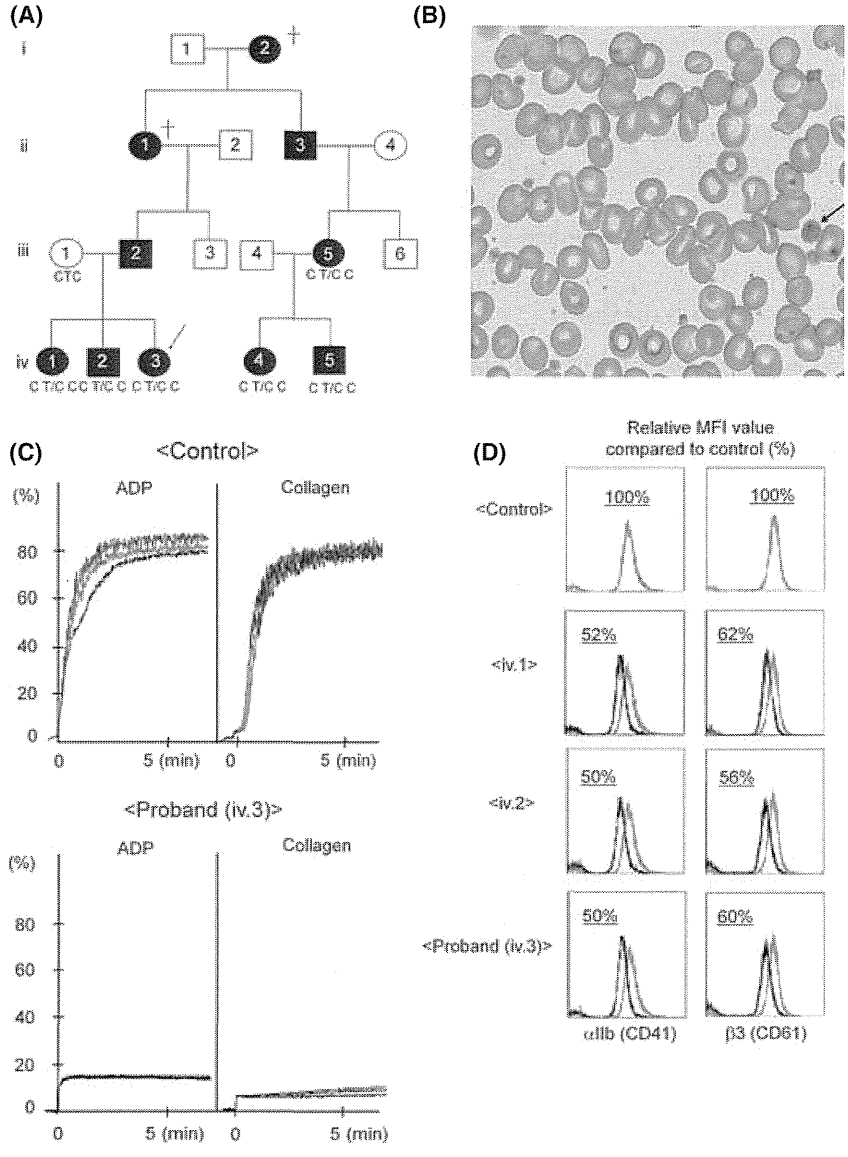

Fig 1. Platelet morphology and aggregation tracings. (A) The pedigree shows affected (filled) and unaffected (open) females (circles) and males (squares). The patient is indicated by an arrow. (B) Platelet morphology as determined by optical microscopy. Peripheral blood specimen obtained from the patient stained with May-Giemsa. The arrow indicates a macrothrombocyte. Original magnification × 600. (C) Representative platelet aggregation tracings in response to ADP and collagen stimuli in platelet-rich plasma from the patient and an unrelated normal control. (D) Flow cytometry of surface integrin αIIb (CD41) and β3 (CD61) expression. Samples were obtained from three affected individuals of the pedigree and an unrelated normal control. Data were calculated as relative MFI value (%), where MFIs of affected individuals were divided by MFI of a control sample.

Exome sequencing

Genomic DNA was obtained from four affected individuals in the pedigree and whole exome sequencing was performed. Briefly, 3 μg genomic DNA was fragmented by Covaris S2 (Covaris, Woburn, MA, USA) and ligated to adaptors, followed by hybridization to biotinylated RNA baits according to the manufacturer's instruction (Agilent Technologies, Santa Clara, CA, USA). The generated sequence tags were sequenced by the 76 bp paired-end protocol of Illumina GAIIx (Illumina, San Diego, CA, USA) and mapped onto the human genomic sequence (hg18, UCSC Genome Browser) using the sequence alignment program Eland (Illumina). Unmapped or redundantly mapped sequences were removed from the data set, and only uniquely mapped sequences were used for further analyses. Positions relative to RefSeq genes were calculated based on the respective genomic coordinates. Genomic coordinates of exons and the protein-coding regions of the RefSeq transcripts are as described in hg18. To verify the presence of *ITGB3* gene alteration, amplification and direct sequencing of a part of exon 14 was performed with the following primers; 5′-C ATAGCCAGTTCAAGTGACTCCTG-3′ for forward primer and 5′-ACGATGGTACTGGCTGAACATGAC-3′ for reverse primer.

Results

Pedigree of a family with autosomal dominant thrombocytopenia with anisocytosis

In the original patient, marked platelet anisocytosis was observed in peripheral blood samples (Fig 1B). Platelet aggregation induced by ADP (1–4 μmol/l) and collagen (0·5–2 μg/ml) was markedly reduced (Fig. 1C and Table I), but agglutination induced by ristocetin (1·25 mg/ml) was within

the normal range (data not shown). Three affected individuals (iii.5, iv.1, and iv.2) showed abnormalities in platelet function similar to those of the original patient. In these affected individuals, the αIIb and β3 expression levels, which were indirectly estimated as relative MFI value (%), were 43–75% of a healthy control (Fig 1D and Table I). The number of αIIbβ3 molecules on the platelet surface in patients, as evaluated by flow cytometry using QIFIKIT, was 35 000–38 400 copies/platelet (MFI: 212·1 –232·4), whereas in an unaffected individual of the pedigree (iii.1) and an unrelated control, there were 65 200 and 62 100 copies/platelet (MFI: 389·2 and 371·3), respectively (Table I). The tendency to bleed was mild to moderate, as exemplified by the following episodes: when family member iv.1 received a bruise to the face, treatment with recombinant Factor VIIa was required because of persistent epistaxis; also, family member iii.5 had had to give birth by Caesarean section because of low platelet count. The family pedigree (Fig 1A), which shows no evidence of consanguineous marriage, strongly suggests the inheritance of thrombocytopenia as an autosomal dominant trait. The laboratory findings are shown in Table I.

Identification of the integrin β3 L718P mutation by whole exome analysis

To isolate a candidate gene alteration responsible for the thrombocytopenia, whole exome sequencing analysis was performed using genomic DNA obtained from the patient (iv.3), her sister and brother (iv.1 and iv.2) and a cousin (iv.4). A total of 794 non-synonymous gene alterations among 1551 SNPs that are not registered in dbSNP 129/130 were detected in the patient. To isolate the responsible gene, we selected non-synonymous gene alterations shared by the four affected individuals as strong candidates. Among the 90 alterations commonly found in the affected individuals of the pedigree (individual numbers of SNPs/mutations are shown in Table II), we focused on the heterozygous non-synonymous T2231C alteration in exon 14 of the *ITGB3* gene, which results in the substitution of leucine at 718 for proline (L718P) in the integrin β3 protein. We selected this because it was recently reported as a candidate mutation responsible for thrombocytopenia (Jayo *et al*, 2010). The presence of the mutation in six affected individuals of the pedigree (iv.1, iv.2, iv.3, iv.4, iii.5 and iv.5) and its absence in an unaffected individual (iii.1) and an unrelated control was confirmed by a direct-sequencing (Fig 2). As far as we could determine, no other non-synonymous gene alterations previously reported to cause thrombocytopenia or defective platelet function were present in the affected individuals of the pedigree. In addition, the L718 residue in integrin β3 is well-conserved between species and amino acid substitution in this position is predicted by bioinformatic tools, including Polyphen and SIFT, to cause a significant change in protein structure and function (data not shown). These observations strongly suggest that the L718P mutation in integrin β3 is the responsible gene alteration that causes familial thrombocytopenia.

Constitutive but partial activation of the αIIbβ3 complex by β3-L718P

To elucidate the effects of the integrin β3-L718P mutation on the activation status of αIIbβ3 complexes in resting or ADP-activated platelets, fresh platelets were analysed by flow cytometry using PAC-1, a ligand-mimicking antibody that specifically recognizes the activated form of the αIIbβ3 complex (Shattil *et al*, 1987).

Resting control platelets from healthy individuals bound PAC-1 with a similar affinity to those treated with RGDS, a peptide which competitively inhibits the binding of ligands for

Table I. Laboratory data of seven individuals of the pedigree.

						Relative MFI value compared to control (%)		αIIbβ3 molecules		Platelet aggregation (%)	
Patient	Sex	Age (years)	Platelet count ($\times 10^9$/l)	MPV (fl)	PDW (%)	αIIb	β3	MFI	copies/platelet	ADP (4 μM)	collagen (2·0 μg/ml)
iii.1	F	37	210	10·2	12·1	110	111	389·2	65 200	NA	NA
iii.5	F	34	38–67	8·5–11·3	10·0–19·0	43	75	NA	NA	15	12
iv.1	F	11	30–43	7·8–11·2	9·7–16·3	52	62	232·4	38 400	16	8
iv.2	M	8	49–64	10·3–11·1	10·1–14·7	50	56	216·4	35 700	23	16
iv.3	F	6	49–72	9·8–10·9	11·1–13·3	50	60	212·1	35 000	12	8
iv.4	F	4	32–59	9·9–10·8	12·3–15·6	NA	NA	NA	NA	NA	NA
iv.5	M	2	28–50	8·9–9·0	18·0–18·4	49	51	NA	NA	NA	NA

MPV, mean platelet volume (normal range: 9·4–12·3 fl); PDW, platelet distribution width (normal range: 9·5–14·8 %); NA, not available.
αIIbβ3 molecules (copies/platelet) were calculated as $10^{(1.022 \times \log(\mathrm{MFI}) + 2.1679)} - 241$ (see *Materials and methods*).

Table II. Number of SNPs/mutations detected by whole exome sequencing.

Case	iv.1	iv.2	iv.3	iv.4
SNP	21 531	21 697	20 413	20 113
Not in dbSNP 129 and 130	1 674	1 722	1 473	1 551
Non-synonymous alternations				
Homozygous	62	58	65	42
Heterozygous	800	815	667	752
Non-synonymous (common)	90			

αIIbβ3 complex such as fibrinogen and PAC-1 (Fig 3A, compare black and blue lines), indicating that wild-type αIIbβ3 in resting platelets is not activated. In contrast, platelets obtained from the affected individuals (iii.5, iv.1, iv.2 and iv.3) showed a slight increase of PAC-1 binding compared to those treated with RGDS (Fig 3A). Indeed, resting platelets from affected individuals showed a slight but significant increase of PAC-1 binding relative to healthy individuals (Fig 3A, top panel). In addition, flow cytometric analysis using FITC-conjugated fibrinogen also showed a significant increase of fibrinogen binding potential in resting platelets from affected individuals compared with healthy controls (bottom panel). Because MPV (shown in Table I) did not exceed the normal range (9·4–12·3 fl) and surface expression levels of αIIbβ3 were lower in patients than controls (Fig 1D), it is proposed that these observations indicate spontaneous activation of αIIbβ3-L718P in resting platelets.

ADP-activated platelets from healthy volunteers, on the other hand, bound to PAC-1 with a very high affinity (Fig 3B, red lines and 3B, top panel), as expected. In contrast, only a small increase of affinity to PAC-1 was observed in ADP-treated platelets carrying the β3-L718P mutation, resulting in a marginal increase of binding potential (bottom panel). These findings suggest that αIIbβ3-L718P is partially activated in the absence of inside-out signals such as ADP, but nevertheless cannot be fully activated in the presence of such signals.

To confirm the contribution of the integrin β3-L718P mutation to spontaneous activation of αIIbβ3, CHO cells were transiently transfected with expression vectors encoding integrin β3-WT, -L718P, -D723H or -T562N together with a vector encoding αIIb-WT. Flow cytometric analysis (Fig 3C) revealed that αIIbβ3-L718P expressed in CHO cells bound to PAC-1 to the same degree as αIIbβ3-D723H, a mutant previously reported to partially activate αIIbβ3, and to a lesser extent than a fully active αIIbβ3-T562N mutant (Kashiwagi *et al*, 1999). We calculated the activation indices (see *Materials and methods*) (Hughes *et al*, 1996; Schaffner-Reckinger *et al*, 2009) of αIIbβ3-L718P and -D723H as 0·23 ± 0·07 and 0·16 ± 0·02, respectively, taking αIIbβ3-T562N as fully active (=1·0) and αIIbβ3-WT as inactive (=0) (Fig 3D). Because CHO cells were not stimulated by ADP in this experiment, each index represents αIIbβ3 activation status at rest.

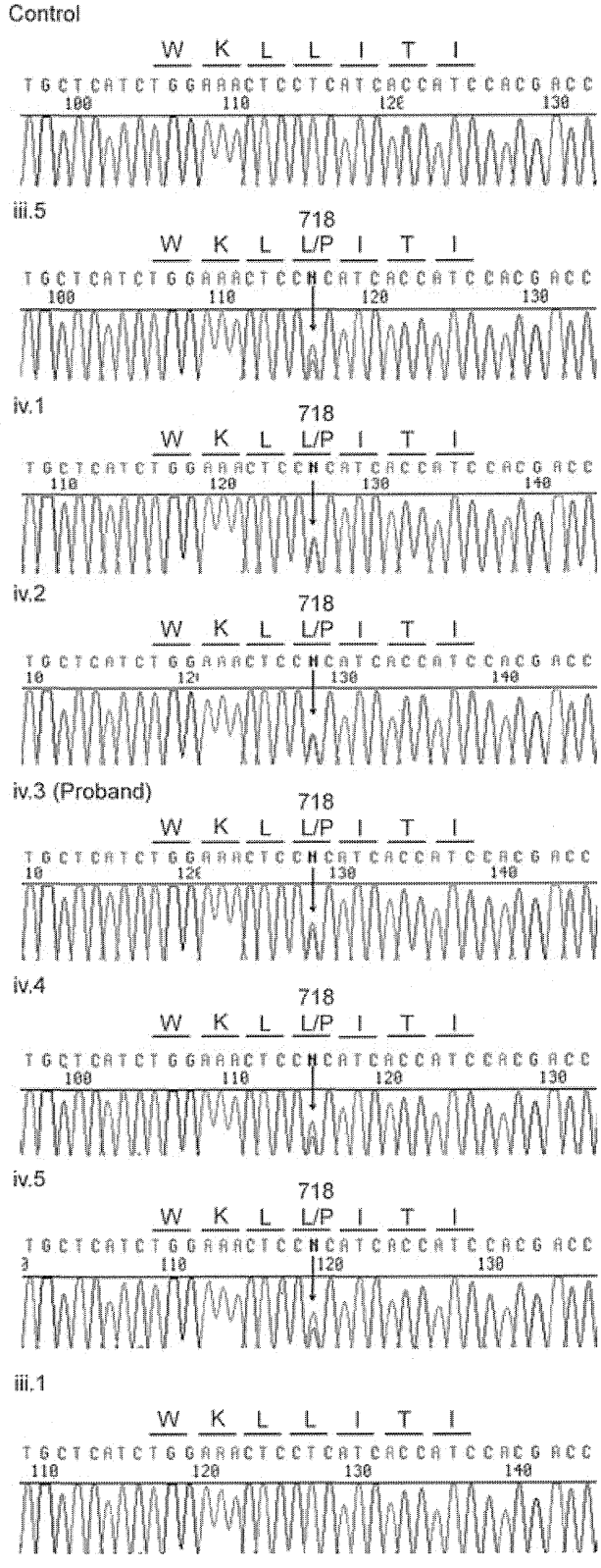

Fig 2. Direct sequencing analysis around T2231 in exon 14 of the *ITGB3* gene. Genomic DNA extracted from the affected and unaffected individuals of the pedigree were amplified by polymerase chain reaction and sequenced. Arrows indicate the position of the T2231 mutation in the *ITGB3* gene.

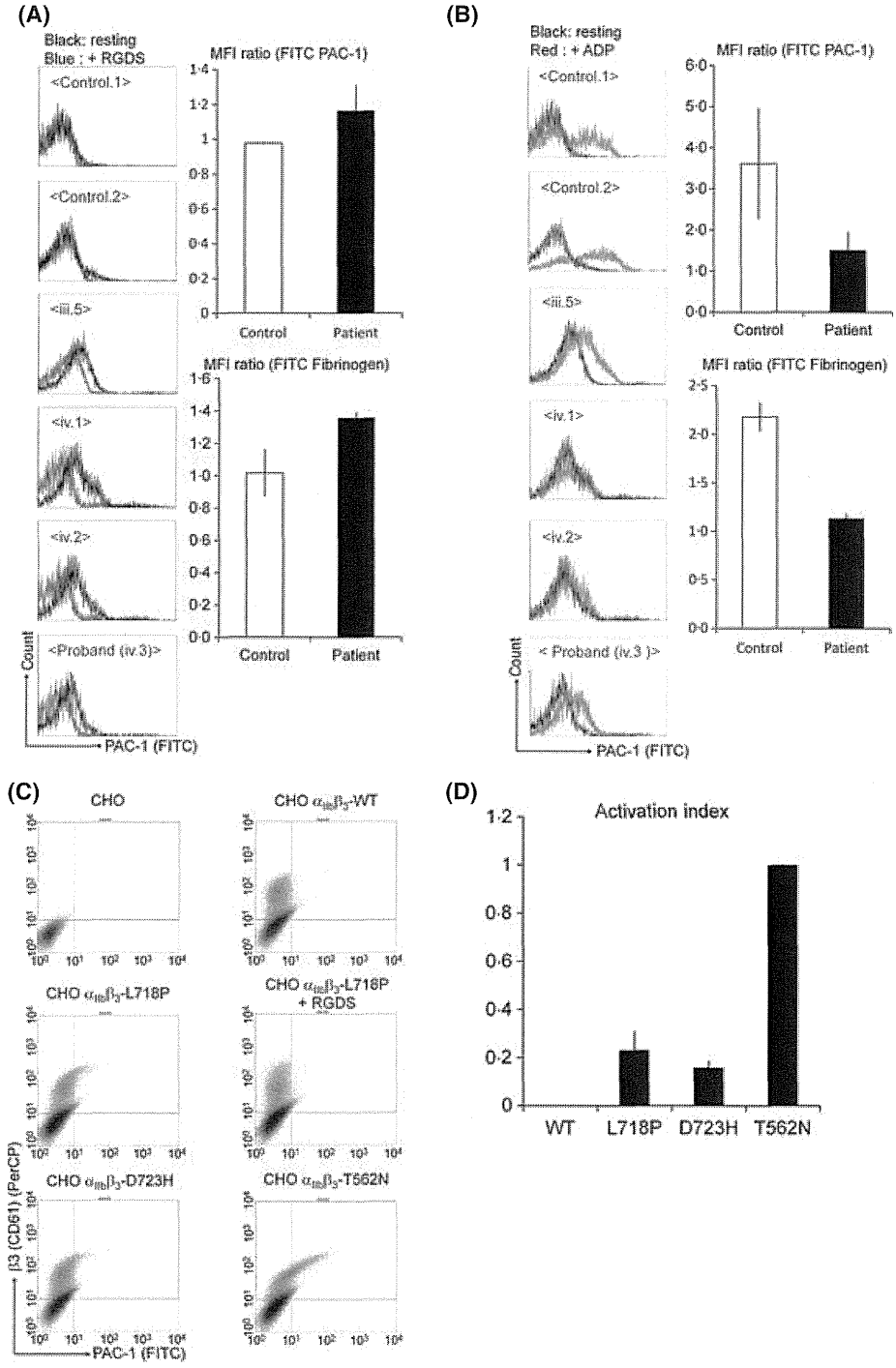

Fig 3. Functional analysis of integrin β3-L718P mutation. (A) Spontaneous binding of PAC-1 antibody to platelets obtained from affected individuals of the pedigree. Non-activated platelets (within 10 min after blood collection), incubated with or without 1 mM RGDS, were stained with FITC-conjugated PAC-1 antibody. After fixation, binding of PAC-1 to platelets was analysed by flow cytometry. Activation status of αIIbβ3 complex on resting platelets bound to FITC-PAC-1 (top) and FITC-fibrinogen (bottom). Mean fluorescence intensity (MFI) ratio was estimated by dividing the MFI of resting platelets by that of resting platelets incubated with RGDS. (B) Reduced activation of αIIbβ3 from affected individuals. The resting and ADP-stimulated platelets, stained with FITC-conjugated PAC-1 antibody were analysed by flow cytometry. Activation status of αIIbβ3 on stimulated platelets bound to FITC-PAC-1 (top) and FITC-fibrinogen (bottom). Values were estimated by dividing the MFI of platelets stimulated with ADP by those of resting platelets. (C) Partial activation of αIIbβ3-L718P and -D723H on CHO cells. CHO cells transfected with αIIbβ3 expression vectors (β3-WT, -L718P, -D723H and -T562N) were seeded on 100 μg/ml fibrinogen-coated coverslips in 6-well dishes. The cells, treated with or without RGDS, were stained with FITC-conjugated PAC-1 antibody and PerCP-conjugated anti-CD61 antibody and analysed by flow cytometry. (D) Activation index of αIIbβ3 mutants. Activation status of CHO cells expressing αIIbβ3-L718P and -D723H was compared with that of αIIbβ3-T562N as described in the "*Materials and methods*".

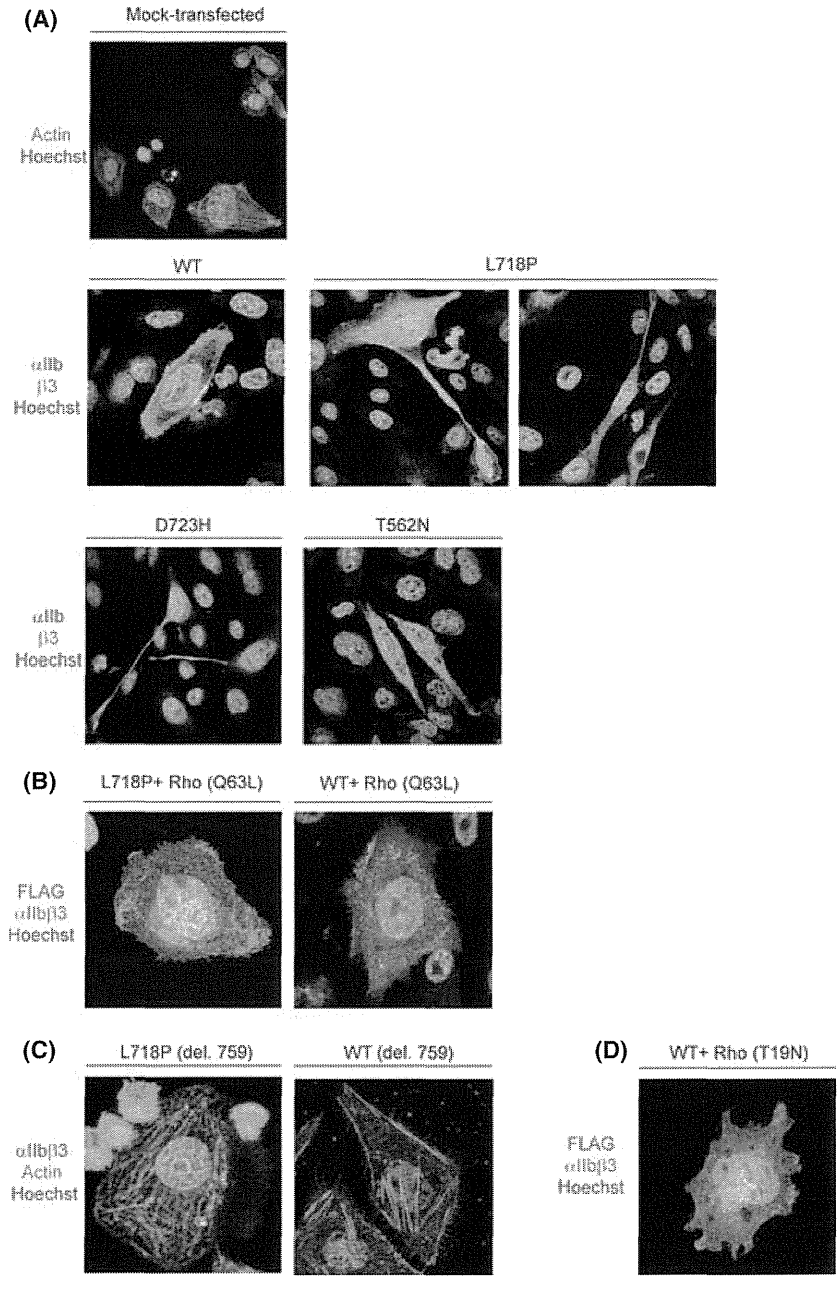

Fig 4. Overexpression of RhoA mutants or integrin β3-L718P (del. 759) modulates the formation of proplatelet-like cell protrusions in CHO cells. (A) Changes in CHO cell morphology by αIIbβ3 mutants. CHO cells transfected with αIIbβ3-L718P, -T562N and -D723H were seeded on fibrinogen-coated coverslips. After an 8-h incubation, the cells were fixed and stained with anti-CD41 and -CD61 antibodies followed by staining with Cy3- and Alexa 488-conjugated secondary antibodies. Mock-transfected cells were stained with Alexa 488-conjugated phalloidin and Hoechst 33342. (B) Inhibition of proplatelet-like protrusion formation by constitutively-active RhoA. An expression vector that encodes FLAG-tagged RhoA (Q63L) was transfected together with αIIbβ3-L718P or -WT expressing vectors into CHO cells. The cells grown on fibrinogen-coated coverslips were fixed and stained with anti-CD41 and anti-DDDDK-tag antibodies followed by staining with Alexa 488- and Cy3-conjugated secondary antibodies. (C) C-terminal deletion of β3-L718P inhibits the formation of proplatelet-like protrusions. C-terminal deleted integrin β3-L718P or -WT (del. 759) was expressed together with αIIb in CHO cells. The cells were fixed and stained with anti-CD41 antibody followed by staining with Cy3-conjugated secondary antibody and Alexa-488-labeled phalloidin. (D) A dominant-negative (T19N) form of RhoA was overexpressed in CHO cells. Images were taken as in (B).

Involvement of RhoA signalling in proplatelet-like protrusion formation

As previously reported by others (Ghevaert *et al*, 2008; Jayo *et al*, 2010), CHO cells expressing αIIbβ3-L718P, as well as αIIbβ D723H, formed long proplatelet-like protrusions on fibrinogen-coated dishes that were not observed in cells expressing wild-type αIIbβ3 (Fig 4A). In contrast, although cells expressing αIIbβ3-T562N, which yields a fully activated conformation (Kashiwagi *et al*, 1999), changed from their original round shape surrounded by a broad protrusion (Fig 4A, mock-transfected) to rhomboid-like cell morphology, proplatelet-like protrusions were rarely seen (Fig 4A). This suggests that mutants partially activating the integrin complex induce long proplatelet-like protrusions.

Recently, it was reported that the formation of proplatelet-like protrusions in CHO cells is mediated by the downregulation of RhoA activity (Chang *et al*, 2007; Schaffner-Reckinger *et al*, 2009), which is initiated by the binding of c-Src to the C-terminal tail (amino acid 760–762, Arg-Gln-Thr; RGT) of integrin β3 (Flevaris *et al*, 2007). We found that the formation of long cell protrusions was inhibited when a constitutively-active form of RhoA (Q63L) was introduced into αIIbβ3-L718P-expressing cells (Fig 4B). In addition, CHO cells expressing αIIbβ3-L718P (del. 759) mutant, which lacks the C-terminal c-Src binding site of in-

tegrin β3 (RGT), did not form any proplatelet-like protrusions (Fig 4C). Given that enforced activation of RhoA caused by introducing RhoA (Q63L), as well as de-repression of RhoA through C-terminal deletion of β3 in cells expressing αIIbβ3-WT, did not induce morphological changes in CHO cells (Figs 4B, C), it is proposed that constitutive inhibition but not activation through the c-terminal of β3 is responsible for the formation of abnormal cell protrusions in L718 mutants. However, as the enforced expression of a dominant negative form of RhoA (T19N) in αIIbβ3-WT expressing cells did not result in typical proplatelet-like protrusions (Fig 4D), this suggests that downregulation of RhoA was required but not sufficient for the formation of proplatelet-like protrusions induced by integrin β3-L718P.

Discussion

We report a pedigree with individuals suffering from a lifelong haemorrhagic syndrome, all of whom were carrying the integrin β3-L718P mutation. This had previously been reported only in a sporadic patient (Jayo *et al*, 2010). Next-generation sequencing, together with the clinical data of the patients, established that this integrin β3-L718P mutation causes thrombocytopenia resembling the disease caused by a different integrin mutation, β3-D723H, although the size of the platelets seems to differ somewhat between these mutations (Ghevaert *et al*, 2008; Schaffner-Reckinger *et al*, 2009).

Considering the dominant inheritance pattern of the haemorrhagic tendency caused by integrin β3-L718P as well as β3-D723H, these would be gain of function mutations, unlike those causing Glanzmann thrombasthenia. Indeed, expression of integrin β3-D723H partially activates the αIIbβ3 complex, resulting in downregulation of RhoA activity and induction of microtubule-dependent proplatelet-like cell protrusions considered relevant for production of macrothrombocytes (Ghevaert *et al*, 2008; Schaffner-Reckinger *et al*, 2009). Integrin β3-L718P appears to act in a similar fashion (Fig 4A and B). Interestingly, we demonstrate that the three C-terminal amino acid residues (RGT) of integrin β3 are required for L718P to form proplatelet-like cell protrusions (Fig 4C). RGT provides a binding site for c-Src tyrosine kinase, which was shown to inactivate RhoA (Flevaris *et al*, 2007), further supporting the hypothesis that integrin β3-L718P plays a role in causing megakaryocytes to produce abnormal platelets through the inhibition of RhoA.

In platelets derived from megakaryocytes that carry the integrin β3-L718P mutation, full activation of αIIbβ3 complex in response to inside-out stimuli is inhibited, as shown by reduced binding of PAC-1 and fibrinogen on stimulation with ADP (Fig 3B). A simple scenario is that, in platelets, integrin β3-L718P acts as a loss of function mutation. However, given that the carriers of Glanzmann's thrombasthenia who have both normal and mutant allele and express reduced amounts of the αIIbβ3 complex, in general show normal platelet aggregation, it is possible that the integrin β3-L718P mutation gains a function that ultimately results in the reduction of inside-out signals.

In summary, identification of a pedigree showing autosomal dominant inheritance leads to a model whereby the integrin β3-L718P mutation contributes to thrombocytopenia accompanied by anisocytosis most likely through gain-of-function mechanisms. Further investigations are necessary to fully elucidate these mechanisms by which this mutation exerts its abnormal effect on thrombocytosis and platelet aggregation.

Acknowledgements

We thank Prof. M. Matsumoto and Ms. M. Sasatani for providing clinical data; Ms. M. Nakamura, Ms. E. Kanai and Ms. R. Tai for excellent technical assistance. This work was partly supported by Grants-in-Aid for Scientific Research from the Ministry of Health, Labour and Welfare of Japan.

Author contributions

H.M., T.I. and M.K. designed the work. Y.K., H.M., A.K., S.O. and M.T. performed experiments and analysed data. S.K. contributed essential materials and interpreted data. M.M and K.N. contributed clinical materials and data. H.M, Y.K. and T.I. wrote the manuscript.

Conflict of interest

The authors declare no competing financial interests.

References

Chang, Y., Auradé, F., Larbret, F., Zhang, Y., Couedic, J.P.L., Momeux, L., Larghero, J., Bertoglio, J., Louache, F., Cramer, E., Vainchenker, W. & Debili, N. (2007) Proplatelet formation is regulated by the Rho/ROCK pathway. *Blood*, **109**, 4229–4236.

Flevaris, P., Stojanovic, A., Gong, H., Chishti, A., Welch, E. & Du, X. (2007) A molecular switch that controls cell spreading and retraction. *Journal of Cell Biology*, **179**, 553–565.

George, J.N., Caen, J.P. & Nurden, A.T. (1990) Glanzmann's thrombasthenia: the spectrum of clinical disease. *Blood*, **75**, 1383–1395.

Ghevaert, C., Salsmann, A., Watkins, N.A., Schaffner-Reckinger, E., Rankin, A., Garner, S.F., Stephans, J., Smith, G.A., Debili, N., Vainchenker, W.de, Groot, P.G., Huntington, J.A., Laffan, M., Kieffer, N. & Ouwehand, W.H. (2008) A non-synonymous SNP in the ITGB3 gene disrupts the conserved membrane-proximal cytoplasmic salt bridge in the αIIbβ3 integrin and cosegregates dominantly with abnormal proplatelet formation and macrothrombocytopenia. *Blood*, **111**, 3407–3414.

Hughes, P.E., Diaz-Gonzalez, F., Leong, L., Wu, C., McDonald, J.A., Shattil, S.J. & Ginsberg, M. H. (1996) Breaking the integrin hinge. A defined structural constraint regulates integrin signaling. *Journal of Biological Chemistry*, **271**, 6571–6574.

Jayo, A., Conde, I., Lastres, P., Martinez, C., Rivera, J., Vicente, V. & Manchón, C.G. (2010) L718P mutation in the membrane-proximal

cytoplasmic tail of β3 promotes abnormal αIIbβ3 clustering and lipid domain coalescence, and associates with a thrombasthenia-like phenotype. *Haematologica*, **95**, 1158–1166.

Kashiwagi, H., Tomiyama, Y., Tadokoro, S., Honda, S., Shiraga, M., Mizutani, H., Honda, M., Kurata, Y., Matsuzawa, Y. & Shattil, S.J. (1999) A mutation in the extracellular cysteine-rich repeat region of the β3 subunit activates integrins αIIbβ3 and αVβ3. *Blood*, **93**, 2559–2568.

Kunishima, S., Kashiwagi, H., Otsu, M., Takayama, N., Eto, K., Onodera, M., Miyajima, Y., Takamatsu, Y., Suzumiya, J., Matsubara, K., Tomiyama, Y. & Saito, H. (2011) Heterozygous ITGA2B R995W mutation inducing constitutive activation of the αIIbβ3 receptor affects proplatelet formation and causes congenital macrothrombocytopenia. *Blood*, **117**, 5479–5484.

Nurden, A.T. (2006) Glanzmann thrombasthenia. *Orphanet Journal of Rare Diseases*, **1**, 10.

Nurden, P. & Nurden, A.T. (2008) Congenital disorders associated with platelet dysfunctions. *Thrombosis and Haemostasis*, **99**, 253–263.

Nurden, A.T., Fiore, M., Nurden, P. & Pillois, X. (2011a) Glanznmann thrombasthenia: a review of ITGA2B and ITGB3 defects with emphasis on variants, phenotype variability, and mouse models. *Blood*, **118**, 5996–6005.

Nurden, A.T., Pillois, X., Fiore, M., Heilig, R. & Nurden, P. (2011b) Glanzmann thrombasthenia-like syndromes associated with macrothrombocytopenias and mutations in the gene encosing the αIIbβ3 integrin. *Seminars in Thrombosis and Hemostasis*, **37**, 698–706.

Schaffner-Reckinger, E., Salsmann, A., Debili, N., Bellis, J., Demey, J., Vainchenker, W., Ouwehand, W.H. & Kieffer, N. (2009) Overexpression of the partially activated αIIbβ3D723H integrin salt bridge mutant downregulates RhoA activity and induces microtubule-dependent proplatelet-like extensions in Chinese hamster ovary cells. *Journal of Thrombosis and Haemostasis*, **7**, 1207–1217.

Shattil, S.J., Cunningham, M. & Hoxie, J.A. (1987) Detection of activated platelets in whole blood using activation-dependent monoclonal antibodies and flow cytometry. *Blood*, **70**, 307–315.

Risk Factor Analysis of Bloodstream Infection in Pediatric Patients After Hematopoietic Stem Cell Transplantation

Takeo Sarashina, MD, Makoto Yoshida, MD, PhD,* Akihiro Iguchi, MD, PhD,† Hitoshi Okubo, MD,* Naohisa Toriumi, MD,* Daisuke Suzuki, MD, PhD,‡ Hirozumi Sano, MD,‡ and Ryoji Kobayashi, MD, PhD‡*

Summary: Bloodstream infection (BSI) is a recognized cause of morbidity and mortality in children after hematopoietic stem cell transplantation (HSCT). However, there are limited reports on BSI after HSCT in pediatric patients in multiple centers. This study was a retrospective cohort analysis of consecutive patients who underwent allogeneic and autologous HSCT at the Department of Paediatrics, Hokkaido University Hospital, between 1988 and 2009; the Department of Paediatrics, Sapporo Hokuyu Hospital, between 2007 and 2009; and the Department of Paediatrics, Asahikawa Medical University, between 1989 and 2009. A total of 277 patients underwent HSCT during the study period. In this multicenter analysis, cases of BSI after HSCT were recorded in the early posttransplant period (within the first 100 d), and BSI was observed in 24 of 277 HSCT patients. Multivariate analysis showed that nonmalignant disease was an independent factor associated with BSI after HSCT (hazard ratio 6.3 for aplastic anemia or Wiskott-Aldrich syndrome patients; confidence interval, 1.4-12.8; $P = 0.012$). We conclude that aplastic anemia and Wiskott-Aldrich syndrome were the novel risk factors for BSI in pediatric patients after HSCT.

Key Words: bloodstream infection, stem cell transplantation, children, risk factor

(*J Pediatr Hematol Oncol* 2013;35:76–80)

Hematopoietic stem cell transplantation (HSCT) improves survival in patients with hematological disorders, malignancies, immunodeficiencies, and inborn errors of metabolism. However, the incidence of complications is high, and therefore, it is essential to develop safe transplantation techniques. Bloodstream infection (BSI) is a common critical complication after HSCT and is associated with significant morbidity and mortality in children.[1,2]

Multiple risk factors are associated with this complication in this particular patient population—profound granulocytopenia, mucositis subsequent to the conditioning regimen, indwelling central venous catheters (CVC), and graft versus host disease (GVHD) are the most important factors. Many studies have noted the high incidence and severity of bacterial and fungal infections, which are often fatal, within 100 days of HSCT.[1–4]

Received for publication November 4, 2011; accepted June 29, 2012.
From the *Department of Paediatrics, Asahikawa Medical University, Asahikawa; †Department of Paediatrics, Hokkaido University Graduate School of Medicine; and ‡Department of Paediatrics, Sapporo Hokuyu Hospital, Sapporo, Japan.
The authors declare no conflict of interest.
Reprints: Takeo Sarashina, MD, Department of Paediatrics, Asahikawa Medical University, Midorigaoka-Higashi 2-1-1-1, Asahikawa 078-8510, Japan (e-mail:sara5p@asahikawa-med.ac.jp).

The aim of this study is to investigate the incidence, clinical features, and risk factors of pediatric patients diagnosed with BSI within 100 days of HSCT at multiple centers across Japan.

MATERIALS AND METHODS

Patient Population and Study Period

This study was a retrospective cohort analysis of consecutive patients who underwent HSCT at the Department of Paediatrics, Hokkaido University Hospital, between February 1988 and November 2009 (no data available from March 2007 and November 2009); the Department of Paediatrics, Sapporo Hokuyu Hospital, between April 2007 and November 2009; and the Department of Paediatrics, the Asahikawa Medical University between June 1989 and November 2009. A total of 277 patients underwent HSCT during the study period; their clinical features are shown in Table 1. The median age was 8 years (range, 0 to 21 y). A total of 169 patients had hematological malignancies (61%), 50 patients had solid tumors (18%), and 58 patients had nonmalignant disease (21%). A standard protocol for supportive care was followed. All patients received antimicrobial prophylaxis with oral polymyxin B sulfate, antifungal prophylaxis with oral amphotericin B, oral fluconazole, or intravenous infusion of micafungin sodium, and antiviral prophylaxis with acyclovir; all prophylactic therapies were maintained at least until engraftment. After engraftment, trimethoprim-sulfamethoxazole was used for prophylaxis of *Pneumocystis jiroveci* pneumonitis. Patients undergoing allogeneic HSCT received intravenous immunoglobulin for the first 4 months after transplantation. CVCs were inserted in all patients and generally removed after engraftment.

Definitions

BSI was defined as the isolation of a single bacterial and fungal pathogen from a blood culture. For bacteria that typically colonize the skin, such as coagulase-negative staphylococci (CNS), corynebacteriae other than *Corynebacterium jeikeium*, and other skin contaminants, at least 2 consecutive positive blood cultures were required. Single-agent BSI was defined as the isolation of a single pathogen from a blood culture. Blood cultures were obtained in response to pyrexia with chills and rigors or clinical signs suggestive of infection such as hypotension, new tachycardia, or change in respiratory status. Pyrexia was defined as development of a temperature of 37.5°C or greater on 2 occasions at least 1 hour apart or a single axillary temperature above 38.0°C. BSIs presenting from the start of the conditioning regimen (day −10 to −7) to day 100 after HSCT were included in the analysis. Date of

TABLE 1. Transplant-specific Characteristics

Age	
Median (y)	8 (0-21)
Sex	
Male	169
Female	108
SCT	
BMT	166
BMT + PBSCT	9
PBSCT	41
CBSCT	61
Donor	
Autologous	51
Related	113 (parent 20)
Unrelated	113
HLA	
Matched	153
1 antigen mismatched	60
2 antigen mismatched	6
3 antigen mismatched	7
Autologous	51
Underlying disease	
Hematological malignancies	169
Acute lymphoid leukemia	81
Acute myeloid leukemia	42
Chronic myeloid leukemia	10
Myelodysplastic syndrome	12
Juvenile myelomonocytic leukemia	11
Non-Hodgkin lymphoma	12
Hodgkin lymphoma	1
Solid tumors	50
Neuroblastoma	20
Rhabdomyosarcoma	10
Yolk sac tumor	5
Hepatoblastoma	2
Ewing sarcoma family of tumor	6
Medulloblastoma	3
Alveolar soft part sarcoma	1
Langerhans cell histiocytosis	1
Brain rhabdoid tumor	1
Granulomatous sarcoma	1
Nonmalignancies	58
Aplastic anemia	33
Wiskott-Aldrich syndrome	5
Kostmann syndrome	3
Severe combined immunodeficiency	3
Chronic granulomatous disease	3
X-linked hyper IgM syndrome	1
Hurler syndrome	3
Hurler Scheie syndrome	1
Hunter syndrome	3
Adrenoleukodystrophy	1
Chronic active Epstein-Barr virus infection	1
Paroxysmal nocturnal hemoglobinuria	1

BMT indicates bone marrow transplantation; CBSCT, cord blood stem cell transplantation; HLA, human leukocyte antigen; PBSCT, peripheral blood stem cell transplantation; SCT, stem cell transplantation.

engraftment was defined as the first of at least 3 consecutive days of an absolute neutrophil count of $>500/mm^3$ after stem cell infusion.

Statistical Analysis

Mann-Whitney U test or χ^2 test was used to compare patients with and without BSI. Analysis of overall survival and event-free survival was performed using the Kaplan-Meier method with differences compared by the log rank test. Multivariate stepwise regression was used to determine the independent effects of variables that showed a significant influence in univariate analysis. Statistical analyses were performed using Dr SPSS II for Windows (Version 11.0.1J; SPSS Japan Inc., Tokyo, Japan).

RESULTS

During the study period, 24 (8.7%) of 277 HSCT patients presented with BSI at the study centers; the clinical features of these patients are summarized in Table 2. The patients were diagnosed with BSI at a median stage of 20 days after HSCT (range, days −3 to 94). BSI occurred in 14 patients with malignant disease, 8 patients with aplastic anemia (AA) (comprising pure red cell aplasia) and 2 patients with Wiskott-Aldrich syndrome (WAS). Twelve patients with related donors, 8 patients with unrelated donors, and 4 patients undergoing autologous HSCT developed BSI. Of the 24 patients with BSI, death was directly attributable to BSI in 4 of the patients [with *Staphylococcus aureus* (methicillin-resistant *S. aureus*), *S. epidermidis*, *Aspergillus* spp., and *Streptococcus pneumoniae*] and to other infectious complications in another 4 patients [with *S. aureus* (methicillin-susceptible *S. aureus*), *S. epidermidis*, α-*Streptococcus*, and *Pseudomonas aeruginosa*]. Of the 24 patients, 16 developed BSI during the preengraftment neutropenic period, and 8 presented with postengraftment BSI. Figure 1 shows the overall survival of patients with or without BSI; survival rates were similar for patients with or without BSI (58.3% vs. 59.2%, respectively; $P = 0.471$).

Microbiology

Table 3 shows BSI isolates in this study. Of the isolates of the 24 cases of BSI, 75% of isolates were gram-positive cocci, the most common of which were coagulase-negative *Staphylococcus* spp. (29%). Gram-negative organisms accounted for 21% and mycoses for 4% of the total isolates. There were no patients with polymicrobial infection in this study. Data were analyzed as of November 1, 2010.

Risk Factors

In the univariate analysis, nonmalignant disease, particularly AA, was associated with an increased risk of BSI after HSCT in children, and was statistically significant (Table 4). Another significant risk factor was the conditioning regimen including antithymocyte globulin (ATG) or excluding etoposide. Sex, stem cell source, timing of HSCT, donor, and GVHD prophylaxis did not correlate with the incidence of BSI. Although there tended to be an association between age and acute GVHD (≥ grade II) with BSI, this was not statistically significant. In the multivariate analysis, nonmalignant disease (hazard ratio, 6.292; confidence interval, 1.368-12.821; $P = 0.012$) remained a risk factor for BSI, whereas there was no association between the conditioning regimen and BSI (Table 5).

DISCUSSION

After HSCT, patients often develop infectious complications due to the functional defects in anti-infective mechanisms. Some of these defects, such as profound neutropenia, and the mucosal changes in the oropharynx and gastrointestinal tract, are specifically related to the conditioning regimen, whereas others are generally associated with the presence of GVHD, drugs used in GVHD control, and the presence of an indwelling CVC throughout the treatment period.

TABLE 2. Clinical Features of Patients With BSI

	Age	Sex	SCT	Donor	Disease	Conditioning	GVHD Prophylaxis	Onset (d)	Pathogens	Survival
1	1	F	A-PBSCT	—	ALL(CR1)	BU + VP16 + CY	—	6	α-*Streptococcus*	A
2	2	F	R-BMT	Sister	ALL(CR1)	BU + VP16 + CY	CsA + shortMTX	0	*Serratia marscescens*	A
3	4	M	R-BMT	Mother	WAS	BU + CY + ATG	CsA + shortMTX	25	*Klebsiella*	A
4	1	M	R-BMT	Sister	WAS	BU + CY	CsA + shortMTX	27	*Staphylococcus aureus*	A
5	8	M	R-BMT	Sister	ALL(CR1)	TBI + VP16 + CY	CsA + shortMTX	7	*Fusobacterium*	A
6	1	F	A-BMT	—	RMS(CR1)	CBDCA + VP16 + THP + Mel	—	1	*S. aureus*	D (sepsis)
7	8	M	U-BMT	Unrelated	AA	TBI + CY + ATG	CsA + shortMTX	4	*S. epidermidis*	A
8	1	M	R-BMT	Father (1 locus mis)	AA	TLI + CY + ALG	CsA + shortMTX	4	α-*Streptococcus*	A
9	18	F	U-BMT	Unrelated	AA	TBI + CY + ATG	Tacro + shortMTX	2	α-*Streptococcus*	D (EBV-LPD)
10	18	M	R-PBSCT	Brother	AA	TBI + ALG	—	29	*Aspergillus*	D (Aspergillosis)
11	17	M	U-BMT	Unrelated	AML(CR1)	TBI + Mel	Tacro + shortMTX	18	*S. epidermidis*	D (cGVHD)
12	4	M	R-CBSCT	Sister (1 locus mis)	AML(CR2)	BU + Mel	CsA + mPSL	63	*S. epidermidis*	A
13	8	M	U-CBSCT	Unrelated (1 locus mis)	JMML(CP2)	TBI + VP16 + CY	CsA + mPSL	3	*S. pneumoniae*	D (meningitis)
14	2	M	R-CBSCT	Sister	JMML(CP1)	BU + FLU + Mel	non prophylaxis	4	*S. epidermidis*	A
15	5	M	R-BMT	Sister	AA	CY + ATG	CsA + shortMTX	8	*S. epidermidis*	A
16	9	F	R-BMT	Father (1 locus mis)	ASPS(non-CR)	TBI + FLU + Mel	Tacro + shortMTX	17	*Enterococcus faecium*	D (aGVHD)
17	3	M	U-BMT	Unrelated (1 locus mis)	AA	TBI + CY + ATG	Tacro + shortMTX	38	α-*Streptococcus*	A
18	4	F	U-BMT	Unrelated (1 locus mis)	AA	TAI + FLU + CY + ATG	Tacro + shortMTX	12	α-*Streptococcus*	A
19	8	M	A-BMT	—	ALL (CR2)	TBI + CY	—	8	*S. epidermidis*	A
20	1	F	U-CBSCT	Unrelated (1 locus mis)	LCH(non-CR)	TBI + CY	CsA + PSL	33	*S. epidermidis*	D (sepsis)
21	15	M	A-PBSCT	—	medulloblastoma (non-CR)	TBI + Mel	—	−3	*P. aeruginosa*	D (VOD)
22	5	F	U-CBSCT	Unrelated (1 locus mis)	ALL (CR2)	TBI + VP16 + CY	CsA + mPSL	87	*S. aureus*	D (relapse)
23	4	M	R-BMT	Brother	Pure red cell aplasia	BU + CY + ATG	Tacro + shortMTX	94	*Corynebacterium*	A
24	6	M	R-BMT	Brother	JMML (CP1)	BU + FLU + Mel	CsA + shortMTX	13	*Enterobacter cloacae*	A

aGVHD indicates acute graft versus host disease; A, alive; AA, aplastic anemia; A-BMT, autologous bone marrow transplantation; ALG, antilymphocyte globulin; ALL, acute lymphocytic leukemia; AML, acute myelogenous leukemia; A-PBSCT, autologous peripheral blood stem cell transplantation; ASPS, alveolar soft part sarcoma; ATG, antithymocyte globulin; BU, busulfan; CBDCA, carboplatin; CP, chronic phase; CR, complete remission; CsA, cyclosporine; CY, cyclophosphamide; D, dead; EBV-LPD, Epstein-Barr virus associated lymphoproliferative disease; FLU, fludarabine; JMML, juvenile myelomonocytic leukemia; LCH, Langerhans cell histiocytosis; Mel, melphalan; MTX, methotrexate; PSL, prednisolone; R-BMT, related bone marrow transplantation; R-CBSCT, related cord blood stem cell transplantation; RMS, rhabdomyosarcoma; R-PBSCT, related peripheral blood stem cell transplantation; SCT, stem cell transplantation; TAI, thoracoabdominal irradiation; Tacro, tacrolimus; TBI, total body irradiation; THP, pirarubicin; TLI, total lymphoid irradiation; U-BMT, unrelated bone marrow transplantation; U-CBSCT, unrelated cord blood stem cell transplantation; mis, mismatch; VOD, veno-occlusive disease; VP16, etoposide; WAS, Wiskott-Aldrich syndrome.

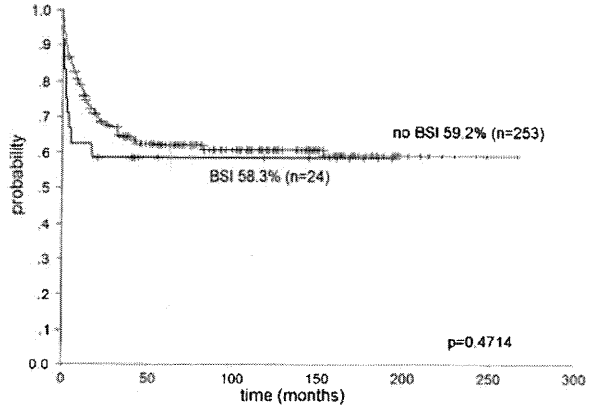

FIGURE 1. Overall Kaplan-Meier analysis of survival after HSCT. Survival rates were similar for patients with and without BSI (58.3% vs. 59.2%, respectively; $P=0.471$).

Previously, the incidence of post-HSCT BSI in children in the early posttransplant period was reported to be 25% to 30%.[1,5] Romano and colleagues reported a higher incidence of BSI with allogeneic rather than with autologous stem cell transplantation. In contrast, Kersun et al[5] reported that race, notably Hispanic and Asian, was the only factor associated with early BSI; however, detailed analyses, including underlying disease, were not recorded.

In our study, the incidence of BSI was less than that in previous reports. This finding could not be attributed to any obvious reason. However, in Japan, many patients with leukemia and solid tumors are hospitalized for chemotherapy. The average hospitalization period of acute lymphocytic leukemia and acute myelogenous leukemia is 5 and 7 months, respectively; therefore, infection control before HSCT was better implemented in our patients than in those of previous reports. So we could identify the novel risk factors for BSI after HSCT in these patients.

We found that the risk factors for BSI after HSCT in children were nonmalignant disease (AA and WAS), ATG regimens, and nonetoposide regimens in univariate analysis. These factors were not identified in previous reports. AA is characterized by pancytopenia, which can result from direct destruction of hematopoietic progenitors, disruption of the marrow microenvironment, or immune-mediated suppression of marrow elements. HSCT is the initial treatment of choice for patients with severe or very severe AA and in most patients with neutropenia. The risk of infection is determined by the patient's neutrophil and monocyte counts[6,7] and the duration of granulocytopenia.[8] WAS, an X-linked recessive syndrome, is characterized by atopic dermatitis, thrombocytopenic purpura with normal-appearing megakaryocytes but small defective platelets, and undue susceptibility to infection. Both diseases are characterized by quantitative or qualitative abnormalities of anti-infective mechanisms. Control of infection is difficult despite hospitalization for the treatment of both diseases; therefore, AA and WAS may be risk factors for BSI in our study. The number of other immunodeficiency patients was

TABLE 3. Organisms Causing BSI

Organism	Frequency (%)
Gram-positive organisms	
S. epidermidis	7 (29)
α-*Streptococcus*	5 (21)
S. aureus	3 (13)
S. pneumonia	1 (4)
Corynebacterium spp.	1 (4)
Gram-negative organisms	
P. aeruginosa	1 (4)
Serratia marscescens	1 (4)
Escherichia coli	1 (4)
Klebsiella spp.	1 (4)
Fusobacterium spp.	1 (4)
Enterobacter cloacae	1 (4)
Fungi	
Aspergillus spp.	1 (4)

TABLE 4. Univariate Analysis of Risk Factors

Factor	BSI (n = 24)	No BSI (n = 253)	*P*
Sex			0.665
Male	16	154	
Female	8	99	
Age (median)	4.5	9.0	0.057
SCT			0.762
BMT	16	150	
BMT + PBSCT	0	9	
PBSCT	3	38	
CBSCT	5	56	
First SCT	21	227	0.726
Second SCT	3	26	
Donor			0.623
Autologous	4	47	
Related	12	101	
Unrelated	8	105	
Parent	3	17	0.394
Alternative donor	9	122	0.393
Disease			**0.016**
Malignant	14	205	
Nonmalignant	10	48	
Year			0.835
-2000	11	122	
2001-	13	131	
Conditioning			
TBI	13	116	0.522
BU	8	75	0.816
Melphalan	7	83	0.822
ATG	9	47	**0.035**
CY	16	147	0.517
etoposide	6	123	**0.032**
Reduced intensity conditioning	6	42	0.207
GVHD prophylaxis			
CsA	12	150	0.394
Tacrolimus	6	37	0.232
MTX	14	146	1.000
mPSL	4	54	0.794
aGVHD (≥ grade II)	2/20	57/206	0.105
Relapse	4	74	0.190
Dead	10	96	0.420
Engraftment	21	233	0.436
Mean time to engraftment (d)	17.87	18.95	0.325

Statistically significant *P*-values are in bold.

aGVHD indicates acute graft versus host disease; ATG, antithymocyte globulin; BMT, bone marrow transplantation; BSI, bloodstream infection; BU, busulfan; CBSCT, cord blood stem cell transplantation; CsA, cyclosporine A; GVHD, graft versus host disease; CY, cyclophosphamide; mPSL, methylprednisolone; MTX, methotrexate; PBSCT, peripheral blood stem cell transplantation; SCT, stem cell transplantation; TBI, total body irradiation.

TABLE 5. Multivariate Analysis of Risk Factors

Factor	HR	P	CI
Disease (nonmalignant)	6.292	**0.012**	1.368-12.821
Without etoposide	0.656	0.418	0.212-1.904
ATG	0.126	0.723	0.421-3.483

Statistically significant *P*-values are in bold.
ATG indicates antithymocyte globulin; CI, confidence interval; HR, hazard ratio.

smaller, so there may be no significant differences between them. In contrast, the use of ATG for immunosuppression has a strong influence on the incidence of infectious complications.[9] In the univariate analysis, ATG regimen was one of the risk factors for BSI, as we expected. However, in the multivariate analysis, the risk factor for BSI was only a nonmalignant disease comprising AA. We hypothesize that occurrence of ATG as a significant risk factor only in the univariate analysis could be because a high proportion of AA patients received ATG in the conditioning regimen.

The most commonly identified organisms in this population were gram-positive cocci, which corresponds with previous reports for both children and adults.[1,5,10–16] *S. epidermidis* is one of many recognized species of CNS affecting or colonizing the human skin, throat, mouth, vagina, and urethra. CNS have been identified to cause infections in patients with indwelling foreign devices, such as CVC. The second most common pathogen was α-*Streptococcus*. A previous report has suggested that empirical treatment with vancomycin before confirmation of positive cultures of α-*Streptococcus* was associated with a trend for decreased mortality.[17] Recently, multiple reports have documented gram-positive cocci as the most commonly diagnosed organism in pediatric patients with hematological disease.

In our study, 1 patient (case 13) experienced *S. pneumoniae* BSI and meningitis, and died on day 6 after HSCT. Pneumococcal infection (PI) is the most common bacterial pathogen, and may cause lethal bacterial infections in late-onset PI after transplantation.[18] In many HSCT patients, functional hyposplenism was seen because of total body irradiation or other conditioning regimens.[18,19] Notably, this patient received a second HSCT, which is significant for PI.

Another important observation is that there was no significant difference in the overall survival of the transplant recipients with and without BSI in the first 100 days after HSCT. Poutsiaka et al[12] reported that BSI after HSCT is associated with increased mortality. In contrast, most of the patients in our study were able to overcome the infection; in addition, there were fewer malignancies in these patients. These factors may result in similar overall survival for our patients with or without BSI.

We have presented a multicenter risk factor analysis for BSI after HSCT in pediatric patients. The incidence of BSI was less than that in previous reports, and we found that nonmalignant diseases (AA and WAS), ATG regimens, and nonetoposide regimens were the novel risk factors for BSI in the early period after HSCT. The clinician should particularly consider pediatric patients associated with these factors to have a higher risk of BSI after HSCT, and thus, plan management strategies accordingly.

REFERENCES

1. Romano V, Castagnola E, Dallorso S, et al. BSIs can develop late(after day 100)and/or in the absence of neutropenia in children receiving allogeneic bone marrow transplantation. *Bone Marrow Transplant.* 1999;23:271–275.
2. Engelhard D. Bacterial and fungal infections in children undergoing bone marrow transplantation. *Bone Marrow Transplant.* 1998;21(suppl. 2):S78–S80.
3. Dell'Orto MG, Rovelli A, Barzaghi A, et al. Febrile complications in the first 100 days after bone marrow transplantation in children: a single center's experience. *Pediatr Hematol Oncol.* 1997;14:335–347.
4. Viscoli C, Castagnola E. Factors predisposing cancer patients to infection. In: Klastersky J, ed. *Infectious Complications of Cancer.* Norwell: Kluwer Academic Publisher; 1995:1–30.
5. Kersun LS, Propert KJ, Lautenbach E, et al. Early bacteremia in pediatric hematopoietic stem cell transplant patients on oral antibiotic prophylaxis. *Pediatr Blood Cancer.* 2005;45:162–169.
6. Bodey GP, Bolivar R, Fainstein V. Infectious complications in leukemic patients. *Semin Hematol.* 1982;19:193–226.
7. Keidan AJ, Tsatalas C, Cohen J, et al. Infective complications of aplastic anemia. *Br J Haematol.* 1986;63:503–508.
8. Hughes WT, Armstrong D, Bodey GP. 2002 guidelines for the use of antimicrobial agents in neutropenic patients with cancer. *Clin Infect Dis.* 2002;34:730–751.
9. Myers GD, Krance RA, Weiss H, et al. Adenovirus infection rates in pediatric recipients of alternate donor allogeneic bone marrow transplants receiving either antithymocyte globulin (ATG) or alemtuzumab (Campath). *Bone Marrow Transplant.* 2005;36:1001–1008.
10. Almyroudis NG, Fuller A, Jakubowski A, et al. Pre-and post-engraftment bloodstream rates and associated mortality in allogeneic hematopoietic stem cell transplant recipients. *Transpl Infect Dis.* 2005;7:11–17.
11. Castagnola E, Bagnasco F, Faraci M, et al. Incidence of bacteremias and invasive mycoses in children undergoing allogeneic hematopoietic stem cell transplantation: single center experience. *Bone Marrow Transplant.* 2008;41:339–347.
12. Poutsiaka DD, Price LL, Ucuzian A, et al. BSI after hematopoietic stem cell transplantation is associated with increased mortality. *Bone Marrow Transplant.* 2007;40:63–70.
13. Junghanss C, Marr KA, Carter RA, et al. Incidence and outcome of bacterial and fungal infections following non-myeloablative compared with myeloablative allogeneic hematopoietic stem cell transplantation: a matched control study. *Biol Blood Marrow Transplant.* 2002;8:512–520.
14. Sayer HG, Longton G, Bowden R, et al. Increased risk of infection in marrow transplant patients receiving methylprednisolone for graft-versus-host disease prevention. *Blood.* 1994;84:1328–1332.
15. Yuen KY, Woo PCY, Hui CH, et al. Unique risk factors for bacteremia in allogeneic bone marrow transplant recipients before and after engraftment. *Bone Marrow Transplant.* 1998;21:1137–1147.
16. Ortega M, Rovira M, Almela M, et al. Bacterial and fungal bloodstream isolates from 796 hematopoietic stem cell transplant recipients between 1991 and 2000. *Ann Hematol.* 2005;84:40–47.
17. Jaffe D, Jakubowski A, Sepkowitz K. Prevention of peritransplantation viridans streptococcal bacteremia with early vancomycin administration: a single-center observational cohort study. *Clin Infect Dis.* 2004;39:1625–1632.
18. Engelhard D, Cordonnier C, Shaw PJ, et al. Early and late invasive pneumococcal infection following stem cell transplantation: a European Bone Marrow Transplantation survey. *Br J Haematol.* 2002;117:444–450.
19. Larry IL. Infectious in asplenic patients. In: Gerald LM, Jorn EB, Raphael D, eds. *Principles and Practice of Infectious Diseases.* 5th ed. Philadelphia: Churchill Livingstone; 2000:3169–3176.

Biochemical and Biophysical Research Communications 417 (2012) 594–600

Contents lists available at SciVerse ScienceDirect

Biochemical and Biophysical Research Communications

journal homepage: www.elsevier.com/locate/ybbrc

TRIM32 promotes retinoic acid receptor α-mediated differentiation in human promyelogenous leukemic cell line HL60

Tomonobu Sato [a,b], Fumihiko Okumura [a], Akihiro Iguchi [b], Tadashi Ariga [b], Shigetsugu Hatakeyama [a,*]

[a] Department of Biochemistry, Hokkaido University Graduate School of Medicine, Sapporo, Hokkaido 060-8638, Japan
[b] Department of Pediatrics, Hokkaido University Graduate School of Medicine, Sapporo 060-8638, Japan

ARTICLE INFO

Article history:
Received 1 December 2011
Available online 11 December 2011

Keywords:
Promyelogenous leukemia
HL60
RARα
TRIM32
Ubiquitin

ABSTRACT

Ubiquitination, one of the posttranslational modifications, appears to be involved in the transcriptional activity of nuclear receptors including retinoic acid receptor α (RARα). We previously reported that an E3 ubiquitin ligase, TRIM32, interacts with several important proteins including RARα and enhances transcriptional activity of RARα in mouse neuroblastoma cells and embryonal carcinoma cells. Retinoic acid (RA), which acts as a ligand to nuclear receptors including RARα, plays crucial roles in development, differentiation, cell cycles and apoptosis. In this study, we found that TRIM32 enhances RARα-mediated transcriptional activity even in the absence of RA and stabilizes RARα in the human promyelogenous leukemic cell line HL60. Moreover, we found that overexpression of TRIM32 in HL60 cells suppresses cellular proliferation and induces granulocytic differentiation even in the absence of RA. These findings suggest that TRIM32 functions as one of the coactivators for RARα-mediated transcription in acute promyelogenous leukemia (APL) cells, and thus TRIM32 may become a potentially therapeutic target for APL.

1. Introduction

Acute promyelogenous leukemia (APL) is a highly malignant subtype of leukemia because of its potentially life-threatening hemorrhagic events due to disseminated intravascular coagulation [1]. One of the most common chromosomal translocations in APL is t(15;17)(q22;q21) resulting in expression of the leukemic-specific chimeric fusion protein PML-RARα [2]. However, the appearance of the differentiating agent all-trans retinoic acid (ATRA), an isoform of retinoic acid, has dramatically improved prognosis of APL [3]. Actually, ATRA likely targets *PML-RARα* gene fusion protein for degradation. Since ATRA therapy showed a high complete remission rate in patients with primary APL and relapsed patients, differentiation therapy with ATRA has now become an established method of treatment in APL [4]. However, the detailed molecular mechanism of ATRA action in APL has not been fully understood.

ATRA plays crucial roles in cell proliferation [5], differentiation [6], tumorigenesis, and in regulation of apoptosis [7]. The biological effects of ATRA are mediated by two types of nuclear receptors: retinoic acid receptors (RARs) and retinoid X receptors (RXRs). Retinoic acid binds to a transcription complex composed of RARs and RXRs, and the heterodimeric pair binds to a specific DNA sequence called a retinoic acid-response element (RARE) [8]. It has been reported that RARs and their fusion proteins such as PML-RARα protein in APL are degraded by the ubiquitin–proteasome pathway [9], which possibly inhibits the complete differentiation of leukemic cells in response to ATRA. On the other hand, there are several reports that ubiquitin-mediated degradation of short-lived regulatory proteins including cell cycle regulatory proteins is essential for ATRA-induced proliferation or differentiation [10,11].

Ubiquitination is a pivotal posttranslational modification system used by eukaryotic cells [12]. It has been reported that gene activities of some nuclear receptors, such as RARs [9,13,14], estrogen receptor [15] and androgen receptor [16,17], are modulated strictly by the ubiquitin–proteasome system, and ubiquitination of those transcriptional factors plays a role not only in the degradation signal but also in the activation signal at a certain transcriptional stage. Tripartite motif (TRIM) proteins are characterized by the presence of a RING finger, one or two zinc-binding motifs called B-boxes, and an associated coiled-coil region (RBCC) [18–20]. It has been reported that TRIM32 has an E3 ligase activity for actin [21], Piasy [22], dysbindin [23], Abi-2 [24], and Argonaute-1 [25]. Point mutation of human TRIM32 has been reported in two genetic disorders: limb-girdle muscular dystrophy type 2H (LGMD2H) [26,27] and Bardet-Biedl syndrome (BBS) [28]. We previously showed that TRIM32 is one of the regulators of RARα by using a comprehensive luciferase reporter assay for *RARE* in neuroblastoma cells [29]. Furthermore, it is important to clarify TRIM32-mediated RARα activity not only in neural differentiation but also in hematopoiesis and leukemogenesis.

* Corresponding author. Address: Department of Biochemistry, Hokkaido University Graduate School of Medicine, Kita 15, Nishi 7, Kita-ku, Sapporo, Hokkaido 060-8638, Japan. Fax: +81 11 706 5169.
E-mail address: hatas@med.hokudai.ac.jp (S. Hatakeyama).

0006-291X/$ - see front matter © 2011 Elsevier Inc. All rights reserved.
doi:10.1016/j.bbrc.2011.12.012

In this study, with the aim of elucidating the molecular function of TRIM32 in promyelogenous leukemic cell differentiation, we analyzed the function of TRIM32 in RARα regulation in the human promyelogenous leukemic cell line HL60. We showed that TRIM32 suppresses cellular proliferation of HL60 cells via transcriptional activation of RARα. We found that TRIM32 acts as a coactivator of RARα not only in neural cell lines but also in human APL cell lines and that overexpression of TRIM32 promotes APL cell differentiation without ATRA, suggesting that TRIM32 is one of the key regulators for APL cell differentiation.

2. Materials and methods

2.1. Cell culture and treatment

HL60, K562, CMK, HEL, KG-1, NKM-1, Namalwa and Jurkat cells (ATCC) were cultured under an atmosphere of 5% CO_2 at 37 °C in RPMI 1640 medium (Sigma) supplemented with 10% fetal bovine serum (Invitrogen). HeLa cells (ATCC) were cultured by the same method in DMEM (Sigma) supplemented with 10% fetal bovine serum (Invitrogen). All-trans retinoic acid (Sigma) was dissolved in dimethyl sulfoxide.

2.2. Cloning of cDNA and plasmid construction

Human *TRIM32* and *RARα* cDNA was isolated and subcloned as previously described [29]. Retinoic acid reporter-luciferase (RAR-Luc) was kindly provided by Dr. Kondo (Hokkaido University).

2.3. Transfection and immunoblot analysis

HL60 cells were electroporated with linearized pCAG-puro-FLAG-TRIM32 plasmid at 275 V and 950 μF once by using Gene Pulser X cell (Bio-Rad Laboratories). HEK293T cells were transfected by the calcium phosphate method. These cell lines were lysed in a solution containing 50 mmol/L Tris–HCl (pH 7.4), 150 mmol/L NaCl, 1% Nonidet P-40, leupeptin (10 μg/mL), 1 mmol/L phenylmethylsulfonyl fluoride, 400 μmol/L Na_3VO_4, 400 μmol/L EDTA, 10 mmol/L NaF, and 10 mmol/L sodium pyrophosphate. The cell lysates were centrifuged at 16,000*g* for 15 min at 4 °C and then boiled in SDS sample buffer. Immunoblot analysis was performed with the following primary antibodies: anti-FLAG (1 μg/mL; M2 or M5, Sigma), anti-HA (1 μg/mL; HA11, Covance), anti-TRIM32 (mouse polyclonal, Abnova), anti-Hsp90 (1 μg/mL; 68, Transduction Laboratories), anti-β-actin (0.2 μg/ml; AC15, Sigma), anti-c-Myc (1 μg/ml; 9E10, Covance) and anti-RARα (Rabbit polyclonal, Cell signaling,). Immune complexes were detected with horseradish peroxidase-conjugated antibodies to mouse or rabbit IgG (1:10,000 dilutions, Promega) and an enhanced chemiluminescence system (GE Healthcare Bioscience Corp).

2.4. Dual-luciferase assay

Cells were seeded in 24-well plates at 1×10^5 cells per well (HEK293T and HeLa cells) and incubated at 37 °C with 5% CO_2 for 48 h. Retinoic acid reporter-luciferase (RAR-Luc) plasmid was transfected with TRIM32 and/or RARα expression vectors into HeLa cells using Fugene HD reagent (Roche). Transfected cells were incubated in DMEM (Sigma) supplemented with 10% fetal bovine serum (Invitrogen) for 24 h and then incubated with ATRA (1 μM) for 24 h, harvested, and assayed for luciferase activity with a Dual-Luciferase Reporter Assay System (Promega). The luminescence was quantified with a luminometer (Promega).

2.5. Cell differentiation assessment and immunofluorescence staining

Smears of mock and TRIM32-transfected HL60 cells were stained with May-Grünwald solution (Merck) for 2 min, rinsed with distilled water, and stained with Giemsa solution (Sigma) for 10 min. Slides were rinsed with distilled water again and air dried. Cell morphology was observed by light microscopy (LABOPHOT, Nikon) under immersion. HL60 cells expressing FLAG-tagged TRIM32 were fixed for 10 min at room temperature with 2% formaldehyde in PBS and then incubated for 1 h at room temperature with a primary antibody to FLAG (Rabbit polyclonal, Sigma) or human CD11b (mouse monoclonal, eBioscience) in phosphate-buffered solution (PBS) containing 0.1% bovine serum albumin. They were then incubated with Alexa488-labeled goat polyclonal antibody to rabbit immunoglobulin or Alexa546-labeled goat polyclonal antibody to mouse immunoglobulin (Molecular Probes) at a dilution of 1:1000 and stained with Hoechst33258. The cells were covered with a drop of VECTASHIELD (VECTOR) and then photographed with a CCD camera (DP71, Olympus) attached to an Olympus BX51 microscope.

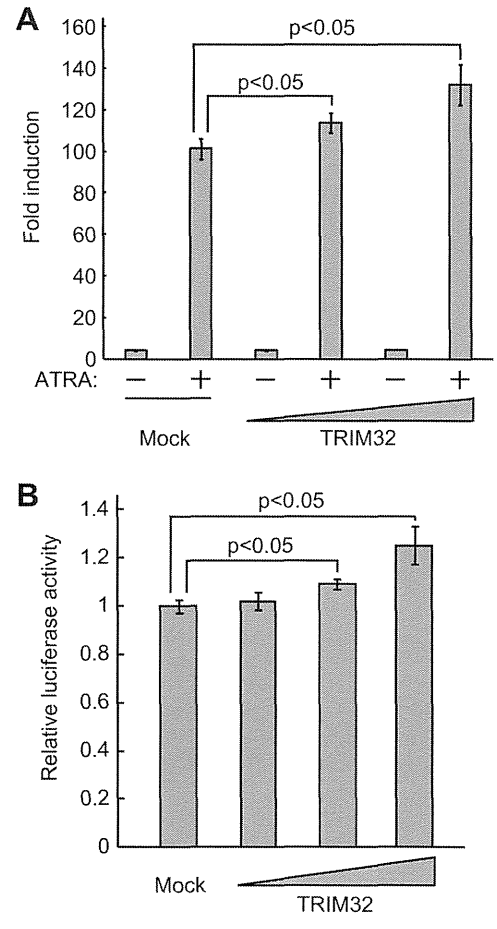

Fig. 1. TRIM32 enhances RARα-mediated transcriptional activity without ATRA. (A) TRIM32 enhances RARα-mediated transcriptional activity in a dose-dependent manner. Expression vectors encoding RARα and TRIM32 or an empty vector with an RAR luciferase reporter vector (RAR-Luc) were transfected into HeLa cells, and then the cells were incubated in a culture medium for 24 h. The cells were incubated with or without ATRA (1 μM) for 24 h and then collected and assayed for luciferase activity. Data are means ± SD of values from three independent experiments. *P* values for the indicated comparisons were determined by Student's *t* test. (B) TRIM32 facilitates RARα-mediated transcriptional activity in a dose-dependent manner without ATRA. RAR-Luc and expression vectors encoding RARα and different amounts of TRIM32 were transfected into HeLa cells. Transfected cells were incubated for 24 h and then incubated without ATRA (1 μM) for 24 h. The cells were then harvested and assayed for luciferase activity.

2.6. Statistical analysis

Student's *t*-test was used to determine the statistical significance of experimental data.

3. Results

3.1. TRIM32 facilitates transcription activity of RARα without ATRA

To determine whether TRIM32 enhances RARα-mediated transcription also in human epithelial carcinoma cell lines, we performed a luciferase reporter assay using an RAR promoter-driven luciferase construct (RAR-Luc) in HeLa cells (Fig. 1A). A TRIM32 expression vector and RAR-Luc were transfected, and luciferase activity was measured with or without ATRA. The luciferase reporter assay showed that TRIM32 facilitates ATRA-dependent RARα-mediated transcriptional activity in a dose-dependent manner in HeLa cells as was found in our previous study using neuroblastoma cells [29] (Fig. 1A). Furthermore, to determine whether TRIM32 in RARα-mediated transcription is dependent on ATRA, we performed a luciferase reporter assay using RAR-Luc without ATRA in HeLa cells. The luciferase reporter assay showed that TRIM32 significantly activates RARα-mediated transcription even without ATRA (Fig. 1B), suggesting that TRIM32 induces differentiation of promyelocytic leukemia cells without ATRA.

3.2. TRIM32 stabilizes the expression level of RARα

It has been reported that *TRIM32* mRNA is expressed in skeletal muscle and in the heart and brain [26]. To clarify the expression profiles of TRIM32 in human leukemic cell lines, we compared the protein levels of TRIM32 by immunoblot analysis in different types of human leukemic cell lines including promyelocytic leukemia cell line HL60, erythroleukemia cell lines K562 and HEL, megakaryocytic leukemia cell line CMK, acute myelogenous leukemia cell lines KG-1 and NKM-1, Burkitt lymphoma cell line Namalwa and T-cell leukemia cell line Jurkat (Fig. 2A). Immunoblot analysis showed that TRIM32 is expressed in various leukemic cell lines regardless of the origins, whereas RARα is highly expressed in promyelocytic leukemia (HL60), erythroleukemia (K562 and HEL) and lymphoblastic leukemia cell lines (Namalwa and Jurkat).

We previously showed that overexpressed TRIM32 physically interacts with RARα in vivo and stabilizes the expression level of RARα in Neuro2a cells and mouse embryonic carcinoma cell line P19. Immunoblot analysis was performed to verify that TRIM32 stabilizes the expression level of RARα not only in neural cell lines but also in HL60 cells without ATRA. An expression vector encoding FLAG-tagged TRIM32 was transiently expressed in HL60 cell lines by electroporation and then immunoblot analysis was performed to evaluate the expression level of endogenous RARα. Immunoblot analysis showed that endogenous RARα was more

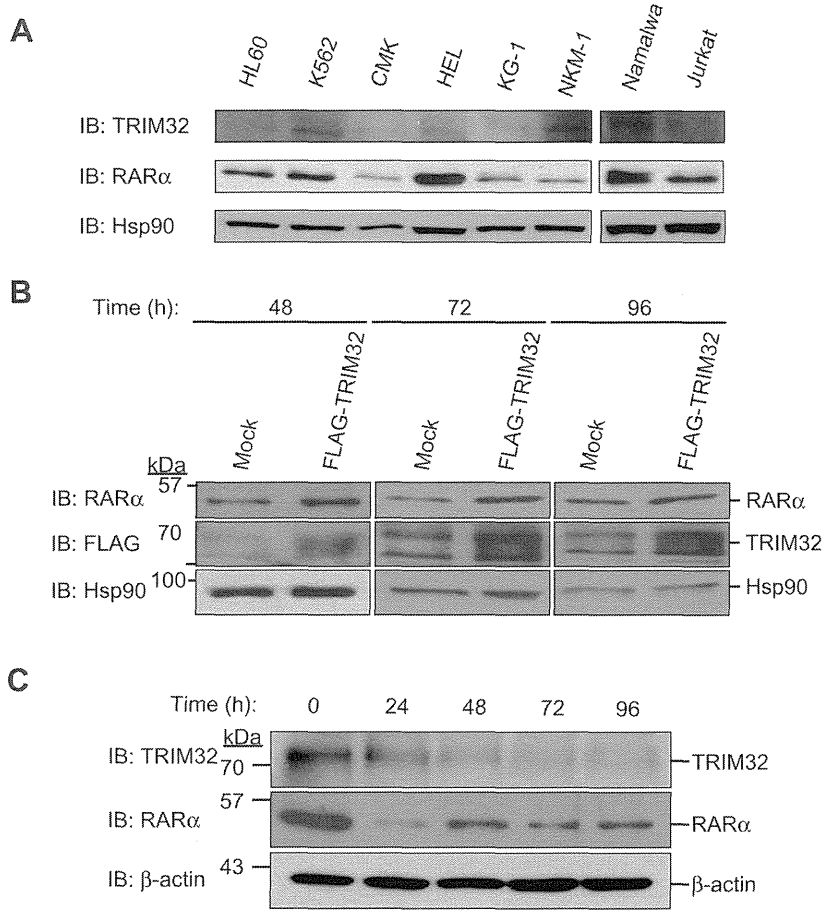

Fig. 2. TRIM32 stabilizes expression levels of RARα. (A) Expression levels of TRIM32 in various human leukemia cell lines. Cell lysates from human leukemia cell lines HL60, K562, CMK, HEL, KG-1, NKM-1, Namalwa, and Jurkat were subjected to immunoblot (IB) analysis with anti-TRIM32, anti-RARα and anti-Hsp90 antibodies. (B) TRIM32 stabilizes expression levels of endogenous RARα. Immunoblot analysis showed expression levels of endogenous RARα in HL60 cells in which FLAG-tagged TRIM32 had been transfected and in mock cells without ATRA. Anti-Hsp90 antibody was used as an internal control. (C) Immunoblot analysis of endogenous TRIM32 and RARα after induction of ATRA in HL60 cells. HL60 cells were seeded at 1×10^6 cells in 60-mm dishes and cultured with ATRA (1 μM). Immunoblot analysis with anti-TRIM32 antibody and anti-RARα antibody was performed at the indicated times after seeding. Anti-β-actin antibody was used as an internal control.